A comparison of the Hull-White model and BGM model

on the EPE of a swap portfolio

J.H. Keim

Technische Universiteit Delft

TU Delft

A comparison of the Hull-White model and BGM model

on the EPE of a swap portfolio

by

J.H. Keim

to obtain the degree of Master of Science
at the Delft University of Technology,
to be defended publicly on T.B.A.

Student number:	4481127	
Project duration:	Jan 4, 2021 – Sep 24, 2021	
Thesis committee:	Prof. dr. ir. C. W. Oosterlee,	TU Delft, supervisor
	Dr. R. Pietersz,	Daily supervisor
	Dr. C. Kraaikamp,	TU Delft
	Dr. R.J. Fokkink,	TU Delft

An electronic version of this thesis is available at `http://repository.tudelft.nl/`.

The cover image is obtained from `https://pixabay.com/nl/`.

TU Delft

Abstract

Interest rate products form a large segment of over-the-counter derivatives. When the interest rate became negative, for the first time, in July 2009, interest rate models needed to adjust. Where first a log-normal model, as the Brace Gątarek Musiela (BGM) model, might have seemed logical for interest-rate products, as they were bounded by zero, now a normally distributed model, as the Hull-White model, could be considered more practical. To our knowledge, no comparison of the Hull-White model and the Brace Gątarek Musiela model has been made on the Expected Positive Exposure (EPE) (and thus Credit Valuation Adjustment (CVA)) of a swap portfolio. Therefore, this thesis compares the Hull-White model with the BGM model on the EPE of a swap portfolio. First, we show how both models can be simulated with Monte Carlo simulation and calibrated to caplets, after which we validate the used simulation. Finally, both models are compared on the convergence, computation time and EPE. It was found that the Hull-White model had a faster convergence and computation time than the BGM model for our implementation. Moreover, it was shown that the Hull-White model and BGM model have significantly different swap EPEs, except for far in-the-money (ITM) swaps and single payment swaps. Therefore, the models used for the EPE of a swap portfolio have a model risk.

Keywords — Hull-White model, Brace Gątarek Musiela (BGM) model, Monte Carlo simulation, Caplet calibration, Expected positive exposure (EPE), Credit valuation adjustment (CVA), Swap portfolio, Model risk

Preface

This master thesis is carried out on behalf of obtaining the Master in Applied Mathematics at the Delft University of Technology. The project is done under the guidance of Raoul Pietersz and the supervision of Cornelis Oosterlee of the department at the Delft Institute of Applied Mathematics. First, I would like to express my gratitude to my daily supervisor, Raoul Pietersz, for the superb supervision, inspirational insights, and valuable feedback. Furthermore, I would like to thank Cornelis Oosterlee for bringing me in contact with this project and for continuous guidance, even when he changed universities, and for the crucial comments in one of the last versions of the report. Last, I would remark my appreciation to Cor Kraaikamp and Robbert Fokkink for making time to be part of my thesis committee for this thesis.

J.H. Keim
Delft, September 2021

Contents

1 Introduction 1

2 Mathematical framework 3
2.1 General theory . . . 3
2.2 Interest-rate products . . . 5
2.3 Credit risk and model risk . . . 7

3 Interest rate modeling 11
3.1 Hull-White model . . . 11
3.1.1 Zero-coupon bond under Hull-White model . . . 12
3.1.2 Zero mean-reversion parameter . . . 13
3.2 Negative rates . . . 13
3.3 Brace Gatarek Musiela (BGM) model . . . 13
3.3.1 Interpolation of the discount factors . . . 15

4 Simulation and calibration 17
4.1 Monte Carlo simulation . . . 17
4.1.1 Hull-White simulation . . . 18
4.1.2 BGM simulation . . . 18
4.2 Calibration . . . 18
4.2.1 Hull-White calibration . . . 19
4.2.2 BGM calibration . . . 20
4.3 Single-curve and multi-curve framework . . . 20

5 Validation of the results 25
5.1 Hull-White model calibration methods . . . 25
5.1.1 Smoothing the curve . . . 27
5.2 Hull-White model and BGM model validation . . . 28
5.3 Validation of the calibration to market curves . . . 28
5.4 Validation EPE and MtM of a swap . . . 29

6 Comparison 33
6.1 Computation . . . 33
6.1.1 Convergence . . . 33
6.1.2 Computational complexity . . . 33
6.2 Comparison . . . 35

7 Conclusion 39

Bibliography 41

A Appendix A: Hull-White parameter theta 43
A.1 Theta parameter with mean-reversion . . . 43
A.2 Theta parameter with zero mean-reversion . . . 44

B Appendix B: Simulation 45
B.1 Simulation Hull-White model with mean-reversion . . . 45
B.1.1 Interest-rate simulation . . . 45
B.1.2 Money-market account simulation . . . 46
B.1.3 Zero-coupon bond simulation . . . 46
B.2 Simulation Hull-White model zero mean-reversion . . . 46
B.2.1 Money-market account simulation . . . 47
B.2.2 Zero-coupon bond simulation . . . 47

C Appendix C: Calibration Hull-White model 49
C.1 Hull-white model calibration to caplets . . . 49
C.2 Jamshidian decomposition . . . 50
C.3 Hull-White model calibration to swaptions . . . 51

D Appendix D: Multi-curve framework 53

Acronyms

ATM At-the-money. 2, 20, 35, 51

AVA Additional valuation adjustment. 9

BGM Brace Gątarek Musiela. iii, xi, 1, 2, 4, 11, 13, 14, 17–22, 25, 28–30, 33, 34, 36–39

CPU Computation time of a task. 34

CVA Credit valuation adjustment. iii, 1, 2, 8, 39

EPE Expected positive exposure. iii, 2, 7, 8, 25, 29–31, 33, 35–40

HJM Heath-Jarrow-Morton framework. 1

ITM In-the-money. 2, 35, 38

MSE Mean squared error. 5, 33

MTM Market-to-market. 2, 25, 29, 30, 33, 35, 36, 39

OTM Out-the-money. 2, 35, 36, 38

PD Probability of default. 8

RR Recovery rate. 8

ZCB Zero-coupon bond. 6, 12

Glossary

$A(t,T)$ The zero-coupon bond can be expressed by $P(t,T) = e^{A(t,T)-B(t,T)r(t)}$, where $A(t,T)$ is defined in equation 3.15. 12

$A_{i,n}(t)$ Annuity factor at time t with first expiry date T_i and last fixed maturity date T_n. 6

$B(t,T)$ The zero-coupon bond can be expressed by $P(t,T) = e^{A(t,T)-B(t,T)r(t)}$, where $B(t,T)$ is defined in equation 3.16. 12

$E(t)$ The positive exposure. 7

$F(t,S,T)$ The simple compounded forward rate at time t with fixing/expiry date S and payment/maturity date T with $0 \leq t \leq S \leq T$. 6

$H(t)$ The pay-off at time t. 3

K Strike or in case of a swap the fixed rate. 6

$M(t)$ The value of the money market account at time t.. 7

N Notional amount. 6

$P(t,T)$ Zero-coupon bond at time t for maturity T. 12

$P^d(t,T)$ Discount zero-coupon bond at time t for maturity T. 20

$P^{f_i}(t,T)$ Forecasting zero-coupon bond at time t for maturity T with $i \in \{1M, 3M, 6M, 12M\}$. 20

$P_{hw}(t,T)$ Simulated Hull-White zero-coupon bond for time t and maturity T. 22

$P_{mkt}(0,T)$ Intial market zero-coupon bond for maturity T. 22, 23

$S(t)$ Security or tradable asset at time t. 3, 6

$S_{i,m,n}(t)$ Swap rate at time t with first expiry date T_i, last floating maturity date T_m and last fixed maturity date T_n. 6, 51

T Maturity time. 6

T_i Expiry/fixing date of, for example, a swap, caplet or floorlet. 7

T_{i+1} Maturity/payment date of, for example, a swap, caplet or floorlet. 7

$V(t)$ Value of a derivative. 3, 7

$V_c(t)$ A call option value. 6

$V_p(t)$ A put option value. 6

$V_{\mathbf{swap}}(t)$ The net present value at time t of a swap. 6

$V_{\mathbf{swpt}}(t,T_i,T_m,T_n)$ Swaption value at time t with first expiry date T_i and last payment dates T_m, T_n. 7

Φ Standard normal cumulative distribution. 7

α Mean-reversion parameter for the Hull-White model. 11, 13

$\mathbb{E}$ Expected value. 3

$\mathbb{Q}$ Risk-neutral measure. 3

μ The mean of a distribution. 4, 5

ω For a payer swap $\omega = 1$ and for a receiver swap $\omega = -1$. 6

σ Volatility. 7

$\sigma_{bgm}(T_i)$ Volatility for the dynamics of the forward rate, $F(t,T_i,T_{i+1})$, in the BGM model. 14, 17, 20

$\sigma_{hw}(t)$ Hull-White model volatility at time t. 11, 17

τ Year fraction between two dates. 6

$\theta(t)$ Hull-White model long term mean parameter. 11, 12

$\tilde{F}(t,S,T)$ The displaced forward rate defined in. 13–15

$\tilde{S}_{i,n}(t)$ The displace swap rate at time t with first expiry date T_i, last floating maturity date T_n and last fixed maturity date T_n. 30

$f^r(t,T)$ The instantaneous forward-rate at time t with maturity T. 6

$m(t)$ The drift term of a stochastic process. 17

$q(t)$ The integer for which, for time t and expiry time T, $T_{q(t)-1} \leq t \geq T_{q(t)}$ holds. 14

$r(t)$ Short-rate. 5, 11

t Time. 3, 5–8

$y(t)$ Defined by the short rate and the mean-reversion. $y(t) = r(t)e^{\alpha t}$. 11

1 Introduction

The financial crisis in 2007/2008 triggered several events. First of all, market participants realised that big companies could have a credit event, like bankruptcy or restructuring. Before the financial crisis, risk management was focused on Counterparty Credit Risk (CCR), which is the loss exposure due to the fact that a counterparty cannot meet its financial obligations. However, this risk was often not included in financial derivatives because of the understanding that large counterparties were too big to fall [14]. To include this risk in the price of financial derivatives, the concept of Credit valuation adjustment (CVA) became more common. CVA is an extra charge on a financial derivative to incorporate the risk that a counterparty is not able to pay its financial obligations. Another effect of the financial crisis was that interest rates were lowered to stimulate the market. The idea behind low-interest rates is that borrowing money is cheap such that people spend more. In this way, central banks try to boost the economy. It even went as far that in July 2009, the central bank of Sweden was the first to implement negative interest rates [22]. Today the European Central Bank has negative interest rates as well. Many interest rate models use a log-normal distribution, which does not allow negative inputs. Therefore, negative interest rates cause a problem for these models. An example of such a model is the Brace Gątarek Musiela (BGM) model [6]. However, for the models that do allow negative interest rates, their disadvantage of negative rates turned into an advantage, as was the case for the Hull-White model, which was first published in 1990 [19].

Interest rate products are a large segment of the market. Known products include mortgages, deposits, loans, pensions, and financial derivatives to hedge risks in fluctuating interest rates, such as interest rate swaps, caps, and floors. In 2019, interest rate derivatives formed around eighty per cent of the global over the counter derivatives [23]. Hence, it should not be surprising that there are a large number of interest rate models. The first couple of stochastic interest rate models regarded the short-rate, which is the interest rate at which one can borrow money for an infinitely small amount of time in the present. A pioneering paper about a short-rate model was the Vasicek model [33] in 1977, which was the first paper to use a mean reversion characteristic. A disadvantage of the model is that it is not able to reproduce the initial interest rate curve, caused by the fact that the model only uses constant parameters. The Ho-Lee model [18] and the Hull-White model [19] introduced extensions of the Vasicek model that allow to choose the parameters in such a way that the initial interest rate curve is reproduced. Before the 2008 financial crisis, negative interest rates were not desirable. Therefore, the Cox-Ingersol-Ross (CIR) model [10] was introduced as an extension of the Vasicek model, a model that does not allow negative interest rates. Another approach of interest rate modelling is to model the instantaneous forward rates, which was first introduced in the Heath-Jarrow-Morton framework (HJM) [17]. Instantaneous forward rates are interest rates taken over an infinitely small amount of time in the future. Another approach was given in 1997 in BGM Model [6], also known as LIBOR Market Model, which simulates the forward rates. The difference between instantaneous forward rates and forward rates is that forward rates are interest rates in the future for a given period instead of for an infinitely small amount of time. The advantage of the BGM model is that the forward rates are directly observable in the market, and the volatilities are directly linked to caplets and floorlets with Black's formula. Caplets (and floorlets) are interest rate derivatives, which are in-the-money if the interest rate exceeds (or is below) a specific, agreed value for a certain date in time. Caplets and floorlets can be seen as options on a reference rate like the LIBOR or EURIBOR rate.

The differences between the short-rate, $r(t)$, instantaneous forward rate, $f^r(t,T_i)$, and the forward rate, $F(t,T_i,T_{i+1})$, is illustrated in Figure 1.1.

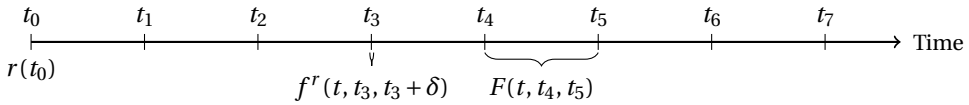

Figure 1.1: An illustration at time $t = t_0$ of the difference between short-rate, $r(t)$, instantaneous forward rate, $f^r(t, T_i) = f^r(t, T_i, T_i + \delta)$ and forward rate, $F(t, T_i, T_{i+1})$. Where δ is an infinitely small number.

Each model has its advantages and disadvantages. Therefore, there are some comparisons made between different interest models. In the papers of [8] and [28], a comparison is made between various short-rate models and (instantaneous) forward rate models. Both papers focus on models that are easy to implement and are used in practice. In [8], the models are compared with interest rate warrants in the German market between 1990 and 1993. Interest rate warrants are options issued by a specific company (not an investor). In this paper, the main valuation criterion is that the model can predict future option prices to measure risk exposure correctly. They find that a two-factor forward rate model best fits this criterion. In [28], the models are compared on the best fit of the market prices of caps using an internally consistent model for a given trading day. The used models for the spot interest rate are Black and Karansinski [4], Pelsser [27] and Hull and White [20] and for the forward rate variations of the Ritchken and Sankarasubramanian model [30]. The paper concludes that all used spot interest rate models outperform the used forward rate models. Furthermore, to our knowledge, no comparison on CVA is made between the short-rate model, the 1-factor Hull-White model, and the forward rate model, the 1-factor BGM model. One of the main drivers of the CVA is the Expected positive exposure (EPE), which is the expected (average) positive credit exposure of a derivative.

Therefore, this thesis aims to compare the Hull-White interest rate model with the Brace Gątarek Musiela (BGM) interest rate model on their Expected positive exposure (EPE) (and Credit valuation adjustment (CVA)).

The aim is to price a swap portfolio through Monte Carlo simulation of the Hull-White model and Brace Gątarek Musiela (BGM) model. Both will be multi-curve, single-currency, 1-factor models. Henceforth, both models will be compared on the computation time of the simulations, the convergence of the Monte Carlo paths and the Expected positive exposure (EPE). The (possible) difference will be displayed for the EPE for ATM, ITM and OTM swaps. The difference will be analysed and explained. Last, a recommendation will be provided on which model is best to use in which situation.

The thesis structure is as follows. In Chapter 2, the mathematical framework is given in which definitions and theorems are stated to provide background information. In Chapter 3, both the Hull-White model and the BGM model are described. In Chapter 4, the simulation and calibration process of both models is presented. The last section of Chapter 4 explains how to incorporate a multi-curve framework (discounting /forecasting curves) in the calibration and simulation. Chapter 5 gives the calibration results and validates that both models price back the market inputs and validates the MTM and EPE of a swap. In Chapter 6, a comparison between the two models is made on convergence, computation time and EPE. Chapter 7 is the conclusion.

2

Mathematical framework

In this section, the mathematical background of the thesis is presented. The information gives an overview of the necessary background knowledge and ensures no misunderstanding regarding definitions will occur.

2.1. General theory

In this section, some theorems and definitions are described regarding the financial market and probability distributions.

Definition 2.1.1 (**Numéraire**)**.** A numéraire is any positive non-dividend paying asset used to measure the value of another tradable asset. In other words, in which units the value of the tradable asset is measured. The standard measure is the risk-neutral measure, $\mathbb{Q}$, which has the money-market account as numéraire.

Definition 2.1.2 (**Arbitrage**)**.** Arbitrage is the event where there is free money in the market by buying/selling certain financial products.

Theorem 2.1.1 (**First fundamental theorem of asset pricing**)**.** If a market is characterised by a risk-neutral measure $\mathbb{Q}$ and a risk-free rate $r(t)$, it does not allow arbitrage [9]. From this theory follows that the value, $V(t)$, at time t of any contingent claim with a payoff, $H(t)$, is given by [26]:

$$V(t) = \mathbb{E}^{\mathbb{Q}}\left[\frac{M(t)}{M(T)}H(T)|\mathscr{F}(t)\right] \tag{2.1}$$

with $\mathbb{E}^{\mathbb{Q}}$ the expected value under the $\mathbb{Q}$-measure.

Definition 2.1.3 (**Change of numéraire**)**.** In a change of numéraire, the numéraire of a tradable asset is changed to another numéraire. Consider a tradable asset, $S(t)$, which is priced under the $\mathbb{Q}^1$-measure with numéraire $M_1(t)$, then:

$$S(t) = \mathbb{E}^{\mathbb{Q}^1}\left[\frac{M_1(t)}{M_1(T)}S(T)|\mathscr{F}(t)\right] \tag{2.2}$$

Henceforth, the Radon–Nikodym is used to change to another numéraire $M_2(t)$ which defines the measure $\mathbb{Q}^2$. The Radon–Nikodym is of the form $\frac{\mathrm{d}\mathbb{Q}^2}{\mathrm{d}\mathbb{Q}^1} = \frac{M_2(t)M_1(T)}{M_2(T)M_1(t)}$. The change from numéraire $M_1(t)$ to numéraire $M_2(t)$ is given by [26]:

$$\begin{aligned}\mathbb{E}^{\mathbb{Q}^1}\left[\frac{M_1(t)}{M_1(T)}S(T)|\mathscr{F}(t)\right] &= \mathbb{E}^{\mathbb{Q}^2}\left[\frac{M_2(t)M_1(T)}{M_2(T)M_1(t)}\frac{M_1(t)}{M_1(T)}S(T)|\mathscr{F}(t)\right] \\ &= \mathbb{E}^{\mathbb{Q}^2}\left[\frac{M_2(t)}{M_2(T)}S(T)|\mathscr{F}(t)\right] \\ &= S(t)\end{aligned} \tag{2.3}$$

which again prices back $S(t)$.

In Chapter 3, the fact that the Hull-White model is an affine process is used to find the closed form solution of the zero-coupon bond.

Definition 2.1.4 (**Affine process**)**.** A process belongs to the class of affine process if the parameters are deterministic functions of time. Take for example a process, $x(t)$, of the form:

$$\mathrm{d}x(t) = \mu(t,x(t))\mathrm{d}t + \sigma(t,x(t))\mathrm{d}W(t) \tag{2.4}$$

$x(t)$ is an affine process if $\mu(t,x(t))$ and $\sigma(t,x(t))$ are of the form

$$\mu(t,x(t)) = \alpha_\mu(t)x(t) + \beta_\mu(t) \tag{2.5}$$

$$\sigma^2(t,x(t)) = \gamma_\sigma(t)x(t) + \delta_\sigma(t) \tag{2.6}$$

Moreover, the discounted characteristic function for $\mathbf{u} \in \mathbb{C}^2$ is given by

$$\phi_{\mathbf{x}}(t,T) = \exp\left(A(t,T) - B(t,T)x(t)\right) \tag{2.7}$$

where A and B satisfy the following Riccati differential equations:

$$\frac{\partial}{\partial t}B(t,T) + \alpha(t)B(t,T) - \frac{1}{2}\gamma(t)B^2(t,T) + 1 = 0 \tag{2.8}$$

$$\frac{\partial}{\partial t}A(t,T) - \beta(t)B(t,T) + \frac{1}{2}\delta(t)B^2(t,T) = 0 \tag{2.9}$$

with $B(T,T) = 0$ and $A(T,T) = 1$. [26]

This thesis will compare the Hull-White model and BGM model. The Hull-White model has normal dynamics, and the BGM has log-normal dynamics. Therefore, we will address details on both distributions and the characteristics these distributions hold.

Definition 2.1.5 (**Normal (or Gaussian) distribution**)**.** The normal distribution is a probability distribution that is symmetrical distributed around the mean μ and has variance σ^2. The probability density function (pdf) evaluated at x is given by [12]

$$\frac{1}{\sigma\sqrt{2\pi}}e^{-\frac{1}{2}\left(\frac{x-\mu}{\sigma}\right)^2} \tag{2.10}$$

Moreover, the cumulative distribution function evaluated at x is given by

$$\int_{-\infty}^{x}\frac{1}{\sigma\sqrt{2\pi}}e^{-\frac{1}{2}\left(\frac{t-\mu}{\sigma}\right)^2}\mathrm{d}t \tag{2.11}$$

with $-\infty < x < \infty$

Definition 2.1.6 (**Standard normal distribution**)**.** The standard normal distribution is the normal distribution with mean $\mu = 0$ and variance $\sigma^2 = 1$. [12] The cumulative distribution becomes

$$\Phi(x) = \int_{-\infty}^{x}\frac{1}{\sqrt{2\pi}}e^{-\frac{1}{2}t^2}\mathrm{d}t \tag{2.12}$$

with $-\infty < x < \infty$

Definition 2.1.7 (**Log-normal distribution**)**.** The log-normal distribution is a probability distribution for which the logarithmic of its random variables are normally distributed; the log-normal random variable X with mean μ and standard deviation σ is defined by the standard normal random variable Z by

$$X = e^{\mu+\sigma Z} \tag{2.13}$$

the probability density function is given by

$$\frac{1}{x\sigma\sqrt{2\pi}}e^{-\frac{1}{2}\left(\frac{\ln(x)-\mu}{\sigma}\right)^2} \tag{2.14}$$

Moreover, the cumulative distribution function is given by

$$\Phi\left(\frac{\ln(x)-\mu}{\sigma}\right) \tag{2.15}$$

with Φ the cumulative distribution function of the standard normal distribution.

The probability density function of the normal and log-normal distribution are shown in Figure 2.1 for different μ and σ^2. For both the normal and log-normal distribution, when, respectively, $\mu = -2.0$ (or $\mu = 2.0$), the centre of the graph shifts two points to the left (or right), and for a larger variance σ^2 the distribution is wider.

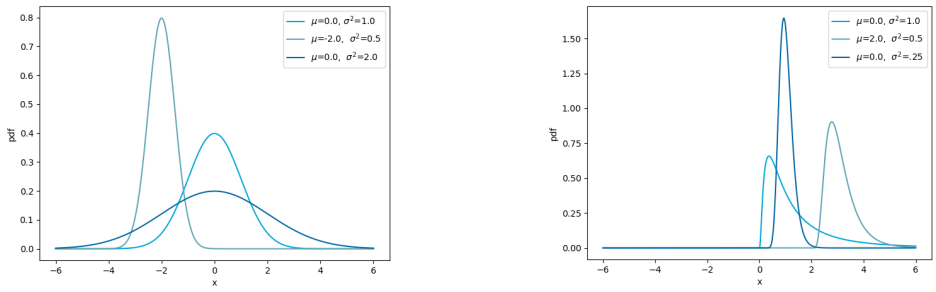

(a) Normal pdf

(b) Log-normal pdf

Figure 2.1: Plots of the probability density function (pdf) for different μ and σ^2 of (a) the normal and (b) log-normal distribution.

Definition 2.1.8 (**Skewness**)**.** Skewness is a measure of asymmetry in a probability distribution. The skewness can be negative, zero, positive or undefined. An example of positive skewness is the log-normal model, which has a right skewed distribution. The skewness can be measured by the third standardised moment given by

$$\text{Skew}(x) = \mathbb{E}\left[\left(\frac{x-\mu}{\sigma}\right)^3\right] \tag{2.16}$$

Since the normal distribution is symmetric, the skewness is zero. [2]

Definition 2.1.9 (**Kurtosis**)**.** The kurtosis is measures the fatness of a tail of a distribution and is given by the fourth standardised moment:

$$\text{Kurt}(x) = \mathbb{E}\left[\left(\frac{x-\mu}{\sigma}\right)^4\right] \tag{2.17}$$

A fat-tailed distribution has a higher kurtosis than that of the normal distribution. The kurtosis of a normal distribution is 3. Therefore, a distribution with a higher kurtosis than 3 is considered fat-tailed. Consequently, extreme events, measured in the tail, have a higher probability for a fat-tailed distribution than that for a normal distribution. [2]

In the validation, the simulated caplet volatilities will be checked against the market volatilities. For the comparison, we will use a confidence interval of 95 %.

Definition 2.1.10 (**Confidence interval**)**.** For mean $\bar{x}$, with known standard deviation s and for n observations, the confidence interval is given by

$$\left[\bar{x} - z^* \frac{s}{\sqrt{n}},\ \bar{x} + z^* \frac{s}{\sqrt{n}}\right] \tag{2.18}$$

With $z^* = \Phi(1-\alpha/2)$, which is 1.96 for a confidence interval of 95% ($\alpha = 0.05$) [12].

Definition 2.1.11 (**Mean-squared error (MSE)**)**.** The mean squared error (MSE) is an error to measure how far an estimate or a simulated value is different from the true value. As the name, mean squared error, suggests; First, the error is squared, then the mean is taken of all the squared errors:

$$MSE = \frac{1}{n}\sum_{i=1}^{n}(y_i - \hat{y}_i)^2 \tag{2.19}$$

with n the number of items, y_i the actual value and $\hat{y}_i$ the estimated or simulated value [12].

2.2. Interest-rate products

This section describes the different interest rate products that are used in this thesis.

Definition 2.2.1 (**Short-rate**)**.** The short-rate, $r(t)$, at time t is the interest rate at which one can earn money on a risk-free investment for an infinitely small amount of time. [26]

Definition 2.2.2 (**Money-market account**)**.** The money-market account, M(t), is the value of a bank account at time t. The process of the money-market account is driven by the short-rate $r(t)$ and defined by:

$$\mathrm{d}M(t) = r(t)M(t)\mathrm{d}t \tag{2.20}$$

with $M(t_0) = 1$. Equation (2.20) has solution:

$$M(t) = e^{\int_{t_0}^{t} r(s)ds} \tag{2.21}$$

Definition 2.2.3 (**Zero-coupon bond**)**.** A zero-coupon bond (ZCB) is an interest rate product that pays 1 currency unit at maturity T. The value of a ZCB is denoted as $P(t,T)$ and is given by

$$P(t,T) = \mathbb{E}^{\mathbb{Q}}\left[\frac{M(t)}{M(T)}P(T,T)|\mathscr{F}(t)\right] = \mathbb{E}^{\mathbb{Q}}\left[e^{-\int_t^T r(z)dz}|\mathscr{F}(t)\right] \tag{2.22}$$

where the fundamental theorem of asset pricing is used and $P(T,T) = 1$. [26]

Definition 2.2.4 (**Instantaneous forward rate**)**.** The instantaneous forward rate, $f^r(t,T)$, at time t with maturity T is defined as:

$$f^r(t,T) = -\frac{\partial}{\partial T}\log P(t,T) \tag{2.23}$$

Moreover, the short-rate can be expressed in terms of the instantaneous forward rate by

$$r(t) = f^r(t,t) \tag{2.24}$$

Definition 2.2.5 ((**Simple compounded**) **forward rate**)**.** The simple compounded forward rate, $F(t,S,T)$, at time t with fixing date S and payment date T with $0 \le t \le S \le T$ is defined as

$$F(t,S,T) = \frac{1}{\tau}\left(\frac{P(t,S)}{P(t,T)} - 1\right) \tag{2.25}$$

where $\tau = T - S$, adjusted to the day count convention.

Definition 2.2.6 (**Reference rate**)**.** A reference rate is a interest rate that is used as benchmark to determine other interest rates, like EURIBOR, EONIA, SOFR.

Definition 2.2.7 (**Interest rate swap**)**.** An interest rate swap (IRS) is a financial derivative that allows two parties to swap a floating interest rate, $\ell(t)$, against a fixed rate, K. In a payer swap, one pays the fixed-rate, and in a receiver swap, one receives the fixed rate. The payoff of an interest rate swap on a payment day $T_{k+1} \in (T_{i+1},\ldots,T_m)$ (assuming payment days for floating and fixed leg are the same) is given by

$$\omega\tau_k N(F(T_k,T_k,T_{k+1}) - K) \tag{2.26}$$

with $\omega = 1$ for a payer swap and $\omega = -1$ for a receiver swap; N the notional amount and $\tau_k = T_{k+1} - T_k$, adjusted to the day count convention. Moreover, the net present value (NPV) of the swap, $V_{\text{swap}}(t)$, for floating payment dates $T_1,\ldots,T_m$ and fixed payment dates $T_1,\ldots,T_n$ is given by

$$V_{\text{swap}}(t) = \omega N\left(\sum_{k=0}^{m-1}\tau_k P(t,T_{k+1})F(t,T_k,T_{k+1}) - K\sum_{l=0}^{n-1}\tau_l P(t,T_{l+1})\right) \tag{2.27}$$

with $P(t,T_{k+1})$ the zero-coupon bond and $F(t,T_k,T_{k+1})$ the forward rate at time t for expiry T_k and maturity T_{k+1}. The swap rate,$S_{i,m,n}(t)$, can be expressed as the strike, K, with a NPV of zero and is given by

$$S_{i,m,n}(t) = \frac{\sum_{k=i}^{m-1}\tau_k P(t,T_{k+1})F(t,T_k,T_{k+1})}{\sum_{k=i}^{n-1}\tau_l P(t,T_{l+1})} \tag{2.28}$$

where the denominator also is known as the annuity factor $A_{i,n}(t)$. Moreover, the swap value can now be given in terms of the swap rate $S_{i,m,n}(t)$ and the $A_{i,n}(t)$ by:

$$V_{\text{swap}}(t) = \omega N A_{i,n}(t)(S_{i,m,n} - K) \tag{2.29}$$

Definition 2.2.8 (**Black Scholes formula**)**.** The Black Scholes formula describes the theoretical value of a call or put option price. The Black Scholes formula for a call option price, $V_c(t)$, and put option price, $V_p(t)$, on a security $S(t)$ with strike K, are given by

$$V_c(t) = S(t)\Phi(d_+) - K\Phi(d_-) \tag{2.30}$$

$$V_p(t) = K\Phi(-d_-) - S(t)\Phi(-d_+) \tag{2.31}$$

$$d_\pm = \frac{\ln(\frac{S(t)}{K}) \pm \frac{1}{2}\sigma^2(T-t)}{\sigma\sqrt{T-t}} \tag{2.32}$$

with $T - t$ the time to expiry, σ the volatility and Φ the cumulative standard normal distribution

Definition 2.2.9 (**Caplet / Floorlet**)**.** Caplet/Floorlet is a financial contract for two time points in the future $T_i < T_{i+1}$, with $\tau_i = T_{i+1} - T_i$, adjusted to the day count convention. The caplet and floorlet values with fixed rated K and notional amount N_i are given by

$$V_i^{CPL}(t, T_i, T_{i+1}) = N_i \tau_i P(t, T_{i+1}) \mathbb{E}^{T_{i+1}} \left[\max(F(t, T_i, T_{i+1}) - K, 0) | \mathscr{F}(t) \right] \tag{2.33}$$

$$V_i^{FL}(t, T_i, T_{i+1}) = N_i \tau_i P(t, T_{i+1}) \mathbb{E}^{T_{i+1}} \left[\max(K - F(t, T_i, T_{i+1}), 0) | \mathscr{F}(t) \right] \tag{2.34}$$

Remark that the expectation is under the T_{i+1}-forward measure instead of the risk-free measure. Hereupon, using Black's formula, the value of the caplet/floorlet at time t becomes:

$$V_i^{CPL}(t) = N_i \tau_i P(t, T_{i+1}) \left(F(t, T_i, T_{i+1}) \Phi(d_+) - K \Phi(d_-) \right) \tag{2.35}$$

$$V_i^{FL}(t) = N_i \tau_i P(t, T_{i+1}) \left(K \Phi(-d_-) - F(t, T_i, T_{i+1}) \Phi(-d_+) \right) \tag{2.36}$$

$$d_\pm = \frac{\ln(\frac{F(t,T_i,T_{i+1})}{K}) \pm \frac{1}{2}\sigma^2 (T_i - t)}{\sigma \sqrt{T_i - t}} \tag{2.37}$$

with Φ the standard normal cumulative distribution function, σ the volatility and $F(t, T_i, T_{i+1})$ the forward rate at time t for expiry date T_i and payment date T_{i+1}.

Definition 2.2.10 (**Swaption**)**.** A swaption is an option on an underlying interest rate swap. In this contract, one has the right, but not an obligation to enter into a specific swap for a predetermined fixed rate K on a future date T_i. The payoff of the swaption is given by

$$\max(V_{\text{swap}}(T_i), 0) \tag{2.38}$$

Moreover, using equation (2.29) the value of the swaption, $V_{\text{swpt}}(t, T_i, T_m, T_n)$, is given under the $\mathbb{Q}$-measure:

$$V_{\text{swpt}}(t, T_i, T_m, T_n) = N \mathbb{E}^{\mathbb{Q}} \left[\frac{A_{i,n}(T_i) M(t_0)}{M(T_i)} \max(\omega(S_{i,m,n} - K), 0) | \mathscr{F}(t) \right] \tag{2.39}$$

with $\omega = 1$ for a payer swap and $\omega = -1$ for a receiver swap. Henceforth, changing to the r $T_{i,n}$-measure, which has $A_{i,n}(t)$ as numéraire, gives

$$V_{\text{swpt}}(t, T_i, T_m, T_n) = N A_{i,n}(t) \mathbb{E}^{T_{i,n}} \left[\max(\omega(S_{i,m,n} - K), 0) | \mathscr{F}(t) \right] \tag{2.40}$$

Now, with Black's formula, follows:

$$V_{\text{swpt}}(t, T_i, T_m, T_n) = N A_{i,n}(t) \left(\omega S_{i,m,n}(t) \Phi(\omega d_+) - \omega K \Phi(\omega d_-) \right) \tag{2.41}$$

$$d_\pm = \frac{\ln(\frac{S_{i,m,n}(t)}{K}) \pm \frac{1}{2}\sigma^2 (T_i - t)}{\sigma \sqrt{T_i - t}} \tag{2.42}$$

with Φ the standard normal cumulative distribution function and σ the volatility.

2.3. Credit risk and model risk

This section discusses counterparty credit risk and model risk. Counterparty risk is the risk that a counterparty will not oblige its obligations. The counterparty risk relevant for this thesis is the different types of exposure and credit valuation adjustment.

Definition 2.3.1 (**Positive Exposure**)**.** The positive exposure is the exposure in the future of a derivative with a specific counterparty. In other words, the value one might be exposed to if another counterparty would go bankrupt. Therefore, the positive exposure, $E(t)$, is defined by

$$E(t) = \max(V(t), 0) \tag{2.43}$$

with $V(t)$ the derivative value. For example, the derivative value for a swap is given in equation (2.27) [26].

Definition 2.3.2 (**Negative Exposure**)**.** The negative exposure is the exposure in the future of a derivative with a specific counterparty. Therefore, the negative exposure is defined by

$$\max(-V(t), 0) \tag{2.44}$$

with $V(t)$ the derivative value [26].

Definition 2.3.3 (**Expected Positive Exposure**)**.** The Expected positive exposure is the expected (average) credit exposure and only considers the positive market values. Exposure can be seen as the money that potentially can be lost if a default of the counterparty occurs. The EPE is defined as:

$$EPE(t_0, t) = \mathbb{E}^{\mathbb{Q}} \left[\frac{M(t_0)}{M(t)} E(t) | \mathscr{F}(t_0) \right] \tag{2.45}$$

with $M(t)$ the money market account and $E(t)$ the (positive) exposure described in equation (2.43) [26].

Moreover, to visualise the difference between the (positive) exposure and expected positive exposure, consider Figure 2.2. Herein, a Monte Carlo simulation with 100 paths of a 10-years receiver swap is given. In Figure (a), the Monte Carlo of the swap value is visualised, in (b), the (positive) exposure and in (c), the expected positive exposure. In section 4.1, we will provide more details of the Monte Carlo simulation.

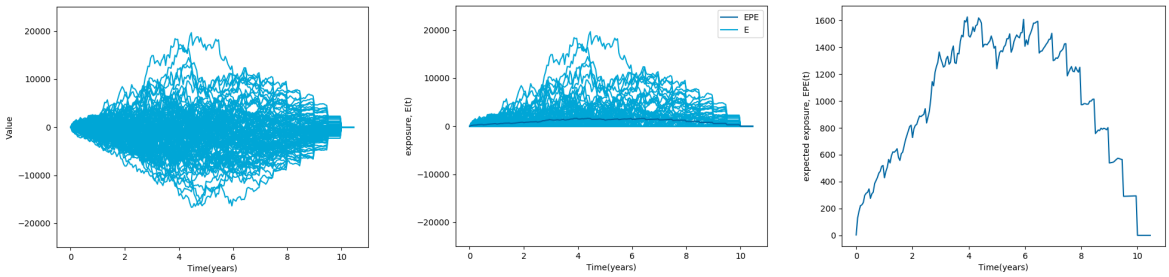

(a) Value (b) Positve exposure (c) Expected positive exposure

Figure 2.2: Plots of a Monte Carlo simulation with 100 paths of a 10-year receiver swap with a semi-annual payments and par strike. In (b) the expected positive exposure from (c) is plotted in dark blue.

Types of exposure In Figure 2.2, a basic example is given where only one derivative, a swap, is considered. However, the EPE can also be calculated for a portfolio. Therefore, we distinguish three types of exposure, according to [26]:

1. **Contract-level exposure**: The exposure of a single derivative, as given in equation (2.43).
2. **Counterparty-level exposure**: The exposure of all derivatives with a single counterparty. The exposure can be found by adding the exposure of all derivatives. For n derivatives with values $V_i(t)$, the counterparty-level exposure is given by

$$\sum_{i=1}^{n} \max\big(V_i(t), 0\big) \tag{2.46}$$

3. **Netting exposure**: The exposure of the different derivatives where the positions offset with each other. The netting exposure of n derivatives with values $V_i(t)$ (that are netted) is given by

$$\max\left(\sum_{i=1}^{n} V_i(t), 0\right) \tag{2.47}$$

Figure 2.3 shows the three described types of exposure for a portfolio of two swaps with 10-year swaps. Swap 1 is a receiver swap with a notional of 100000, and swap 2 is a payer swap with a notional of 50000. The EPE is calculated with a Monte Carlo simulation of 10000 paths.

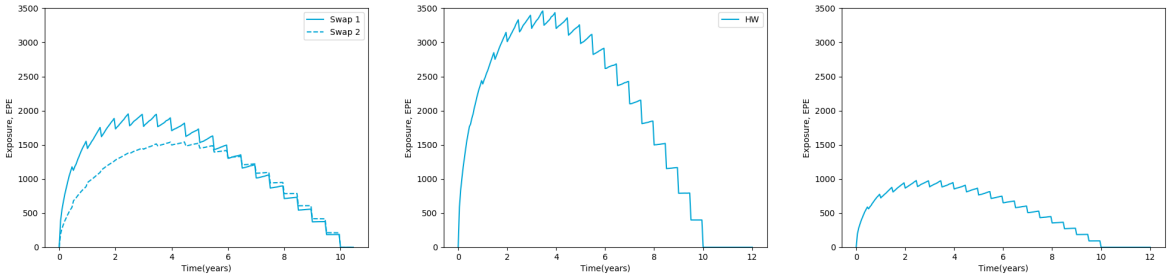

(a) Contract-level exposure (b) Counterparty-level exposure (c) Netting exposure

Figure 2.3: Plots of exposure of two swaps with 10-year swaps with semi-annual payments. Swap 1 is a receiver swap with a notional of 100000, and swap 2 is a payer swap with a notional of 50000. The EPE is calculated with a Monte Carlo simulation of 10000 paths.

Definition 2.3.4 (Credit Valuation Adjustment). The Credit valuation adjustment (CVA) is the extra charge on a derivative to integrate the counterparty risk. In other words, the CVA is the expected loss due to future counterparty default. The CVA is calculated by multiplying the loss given default (one minus the recovery rate), probability of default and the EPE and is defined by:

$$CVA(t_0, T) = (1 - RR) \int_{t_0}^{T} EPE(t) \mathrm{d}PD(t_0, t) \tag{2.48}$$

with RR the recovery rate and PD(s, t) the probability of counterparty default at between time s and t.

Definition 2.3.5 (**Model Risk**)**.** Model risk is a broad term for the various risk that occurs when using and choosing a model. In this thesis, we use the definition of model risk describes in [11]; How different models, which all price back market instruments, can give different risk forecasts.

Definition 2.3.6 (**Additional valuation adjustment (AVA)**)**.** Additional valuation adjustment (AVA) is the difference between the fair value and the prudent value. AVA is used in the calculation of capital reserve requirement of a bank and exists out of number of components. One of those components is the model risk AVA, which quantifies the risks of different models [13].

3

Interest rate modeling

In this chapter, the one-factor Hull-White short-rate model is presented. Moreover, the effect of negative interest rates is discussed and the Brace Gątarek Musiela Model is explained.

3.1. Hull-White model

The one-factor Hull-White model is a short-rate model, which is driven by a mean-reverting process. The dynamics of the Hull-white model are given by [19]

$$\mathrm{d}r(t) = (\theta(t) - \alpha r(t))\mathrm{d}t + \sigma_{hw}(t)\mathrm{d}W(t) \tag{3.1}$$

with α the constant mean-reversion parameter and $\mathrm{d}W(t)$ a Brownian motion under the risk-neutral measure $\mathbb{Q}$; $\sigma_{hw}(t)$ is the short-rate volatility; $\theta(t)$ the long-term mean to which the interest rate, $r(t)$, reverts. In [15], different calibration techniques are discussed. The trade-off is made between a model that perfectly fits the observed calibration inputs and a stable optimisation procedure. The authors conclude that a constant mean-reversion parameter, α, and time-varying volatility, $\sigma_{hw}(t)$, provide a good balance between fitting and stability. The mean-reversion parameter is chosen a-priori and the calibration of the volatility will be discussed in section 4.2.1.

To obtain an analytical expression for $r(t)$, Itô's Lemma is used with $y(t) = r(t)e^{\alpha t}$. It follows that $\mathrm{d}y(t)$ is given by

$$\begin{aligned}\mathrm{d}y(t) &= \frac{\partial y(t)}{\partial t}\mathrm{d}t + \frac{\partial y(t)}{\partial r(t)}\mathrm{d}r(t) \\ &= \alpha r(t)e^{\alpha t}\mathrm{d}t + e^{\alpha t}\mathrm{d}r(t)\end{aligned} \tag{3.2}$$

Now using equation (3.1) we find

$$\mathrm{d}y(t) = e^{\alpha t}\left(\theta(t)\mathrm{d}t + \sigma_{hw}(t)\mathrm{d}W(t)\right) \tag{3.3}$$

Integrating equation (3.3) gives

$$y(t) = y(t_0) + \int_{t_0}^{t} \theta(s)e^{\alpha s}\mathrm{d}s + \int_{t_0}^{t} \sigma_{hw}(s)e^{\alpha s}\mathrm{d}W(s) \tag{3.4}$$

Substitution of $y(t) = r(t)e^{\alpha t}$ in equation (3.4) gives

$$r(t) = r(t_0)e^{-\alpha(t-t_0)} + e^{-\alpha t}\int_{t_0}^{t} \theta(s)e^{\alpha s}\mathrm{d}s + e^{-\alpha t}\int_{t_0}^{t} \sigma_{hw}(s)e^{\alpha s}\mathrm{d}W(s) \tag{3.5}$$

Since the increments of a Brownian motion have a normal distribution, we find that the short-rate, $r(t)$, has a normal distribution with mean

$$\mathbb{E}[\,r(t)|\mathscr{F}_{t_0}] = r(t_0)e^{-\alpha(t-t_0)} + \int_{t_0}^{t} \theta(s)e^{-\alpha(t-s)}\mathrm{d}s \tag{3.6}$$

For the variance the Itô's isometry property is used stated by:

Theorem 3.1.1 (Itô's isometry)**.** Itô's isometry theorem states that for a Brownian motion $W(t)$ and stochastic process $g(t)$ [26]

$$\mathbb{E}\left[\left(\int_{t_0}^{T} g(t)\mathrm{d}W(t)\right)^2\right] = \int_{t_0}^{T} \mathbb{E}\left[g^2(t)\right]\mathrm{d}t \tag{3.7}$$

Using Itô's isometry the variance for r(t) is given by

$$\mathrm{Var}\left[\, r(t)|\mathscr{F}_{t_0}\right] = \int_{t_0}^{t} \sigma_{hw}^2(s) e^{-2\alpha(t-s)} \mathrm{d}s \tag{3.8}$$

Moreover, the term $\theta(t)$ is chosen in such a way to fit the initial term structure. Therefore, for θ we find a time-dependent equation, defined by the instantaneous forward rate at time 0 [7]

$$\theta(t) = \frac{\partial f^r(t_0,t)}{\partial t} + \alpha f^r(t_0,t) + \int_{t_0}^{t} \sigma_{hw}^2(s) e^{-2\alpha(t-s)} \mathrm{d}s \tag{3.9}$$

Appendix A explains how the formula of $\theta(t)$ is obtained.

3.1.1. Zero-coupon bond under Hull-White model

The ZCB is given in definition 2.22 by

$$P(t,T) = \mathbb{E}\left[\exp\left(-\int_t^T r(s)\mathrm{d}s \right) \middle| \mathscr{F}_t \right] \tag{3.10}$$

Since the Hull-White model belongs to the class of affine processes [26], $P(t,T)$ can be defined in terms of $A(t,T)$ and $B(t,T)$ by

$$P(t,T) = \exp\left(A(t,T) + B(t,T) r(t)\right) \tag{3.11}$$

Henceforth, to find $A(t,T)$ and $B(t,T)$ consider the integration of equation (3.5):

$$\begin{aligned}
\int_t^T r(u)\mathrm{d}u &= r(t)\int_t^T e^{-\alpha(u-t)}\mathrm{d}u + \int_t^T \int_t^u \theta(s) e^{-\alpha(u-s)} \mathrm{d}s\mathrm{d}u + \int_t^T \int_t^u \sigma_{hw}(s) e^{-\alpha(u-s)} \mathrm{d}W(s)\mathrm{d}u \\
&= \frac{r(t)}{\alpha}\left(-e^{-\alpha(T-t)}+1\right) + \int_t^T \frac{\theta(s)}{\alpha}\left(-e^{-\alpha(T-s)}+1\right)\mathrm{d}s + \int_t^T \frac{\sigma_{hw}(s)}{\alpha}\left(-e^{-\alpha(T-s)}+1\right)\mathrm{d}W(s)
\end{aligned} \tag{3.12}$$

where in the second line the integral of s and u are interchanged. Inserting this in equation (3.10) gives

$$\begin{aligned}
P(t,T) &= \mathbb{E}\left[\exp\left(-\int_t^T r(s)\mathrm{d}s \right) \middle| \mathscr{F}_t \right] \\
&= \mathbb{E}\left[\exp\left(\frac{r(t)}{\alpha}\left(e^{-\alpha(T-t)}-1\right) + \int_t^T \frac{\theta(s)}{\alpha}\left(e^{-\alpha(T-s)}-1\right)\mathrm{d}s + \int_t^T \frac{\sigma_{hw}(s)}{\alpha}\left(e^{-\alpha(T-s)}-1\right)\mathrm{d}W(s) \right) \middle| \mathscr{F}_t \right] \\
&= \exp\left(\frac{r(t)}{\alpha}\left(e^{-\alpha(T-t)}-1\right) + \int_t^T \frac{\theta(s)}{\alpha}\left(e^{-\alpha(T-s)}-1\right)\mathrm{d}s + \frac{1}{2}\int_t^T \left(\frac{\sigma_{hw}(s)}{\alpha}\left(e^{-\alpha(T-s)}-1\right)\right)^2 \mathrm{d}s \right)
\end{aligned} \tag{3.13}$$

where in the third term itô's isometry is used.

Therefore, $P(t,T)$ can be written as

$$P(t,T) = \exp\left(A(t,T) + B(t,T) r(t)\right) \tag{3.14}$$

with $A(t,T)$ defined as

$$A(t,T) = \int_t^T \theta(s) B(s,T)\mathrm{d}s + \frac{1}{2}\int_t^T \sigma_{hw}(s)^2 B(s,T)^2 \mathrm{d}s \tag{3.15}$$

and $B(t,T)$ as

$$B(t,T) = \frac{1}{\alpha}\left(e^{-\alpha(T-t)}-1\right) \tag{3.16}$$

Moreover, the ZCB is log-normally distributed with SDE [15]

$$\frac{\mathrm{d}P(t,T)}{P(t,T)} = r(t)dt + \sigma_{hw}(t) B(t,T) \mathrm{d}W(t) \tag{3.17}$$

To find a closed-form solution for the integrated variance we consider the bond ratio between the fixing date, S, and payment date, T with $t \le S < T$. In the T -forward measure, this has the dynamics

$$\mathrm{d}\frac{P(t,S)}{P(t,T)} = \frac{P(t,S)}{P(t,T)} \sigma_{hw}(t)\left(B(t,S) - B(t,T)\right)\mathrm{d}W^T(t) \tag{3.18}$$

with integrated variance

$$\begin{aligned}
\mathrm{Var}[P(S,T)|\mathscr{F}_t] &= \int_t^S \sigma_{hw}^2(u)\left(B(u,S)-B(u,T)\right)^2 \mathrm{d}u \\
&= \int_t^S \sigma_{hw}^2(u)\left(\frac{1}{\alpha}\left(e^{-\alpha(S-u)} - e^{-\alpha(T-u)}\right)\right)^2 \mathrm{d}u \\
&= \int_t^S \sigma_{hw}^2(u) e^{-2\alpha(S-u)}\left(\frac{1}{\alpha^2}\left(1 - 2e^{-\alpha(T-S)} + e^{-2\alpha(T-S)}\right)\right)\mathrm{d}u \\
&= \mathrm{Var}\left[r(S)|\mathscr{F}_t\right]\left(\frac{1}{\alpha}(e^{-\alpha(T-S)}-1)\right)^2
\end{aligned} \tag{3.19}$$

Note that $\left(\frac{1}{\alpha}(e^{-\alpha(T-S)}-1)\right)^2 = B(S,T)^2$, with $B(t,T)$ defined in equation (3.16). The integrated variance is used in Black's formula for zero-coupon bond options. In section 4.2, this will be used for calibration of the volatility parameter.

3.1.2. Zero mean-reversion parameter

We want to compare both models in a similar setting. Since the BGM model does not contain a mean-reversion parameter, the mean-reversion parameter, α, of the Hull-White model is chosen to be zero.

The short-rate dynamics with a mean-reversion parameter of zero become

$$\mathrm{d}r(t) = \theta(t)\mathrm{d}t + \sigma_{hw}(t)\mathrm{d}W(t) \tag{3.20}$$

with long-term mean

$$\theta(t) = \frac{\partial f^r(0,t)}{\partial t} + \int_{t_0}^{t} \sigma_{hw}^2(s)\mathrm{d}s \tag{3.21}$$

The derivation of the long-term mean is given in appendix A.2. The integrate short-rate dynamics are given by

$$r(t) = r(t_0) + \int_{t_0}^{t} \theta(s)\mathrm{d}s + \int_{t_0}^{t} \sigma_{hw}(s)\mathrm{d}W(s) \tag{3.22}$$

The integrate short-rate is given by

$$\begin{aligned}\int_t^T r(u)\mathrm{d}u &= r(t)\int_t^T \mathrm{d}u + \int_t^T\int_t^u \theta(s)\mathrm{d}s\mathrm{d}u + \int_t^T\int_t^u \sigma_{hw}(s)\mathrm{d}W(s)\mathrm{d}u \\ &= r(t)(T-t) + \int_t^T \theta(s)(T-s)\mathrm{d}s + \int_t^T \sigma_{hw}(s)(T-s)\mathrm{d}W(s)\end{aligned} \tag{3.23}$$

Therefore, $A(t,T)$ and $B(t,T)$ in equation (3.14) are given by

$$A(t,T) = -\int_t^T \theta(s)(T-s)\mathrm{d}s + \frac{1}{2}\int_t^T \sigma_{hw}^2(s)(T-s)^2\mathrm{d}s \tag{3.24}$$

$$B(t,T) = -(T-t) \tag{3.25}$$

Furthermore, the integrated zero-coupon bond variance with a zero mean-reversion parameter becomes, using equation (3.26) and (3.25):

$$\mathrm{Var}[P(S,T)|\mathscr{F}_t] = \mathrm{Var}\left[r(S)|\mathscr{F}_t\right](T-S)^2 \tag{3.26}$$

3.2. Negative rates

Since negative interest rates are occurring more and more often, some interest rate models need adjustments. The Hull-White model allows negative rates. However, Black's formula for pricing derivatives does not allow negative rates due to the logarithmic term. Therefore, a shifted Black model is used, of the form:

$$V_i^{CPL}(t) = N_i\tau_i P(t,T)\left((F(t,S,T)+\delta)\Phi(d_+) - (K+\delta)\Phi(d_-)\right) \tag{3.27}$$

$$V_i^{FL}(t) = N_i\tau_i P(t,T)\left((K+\delta)\Phi(-d_-) - (F(t,S,T)+\delta)\Phi(-d_+)\right) \tag{3.28}$$

$$d_\pm = \frac{\ln((\frac{F(t,S,T)+\delta)}{(K+\delta)}) \pm \frac{1}{2}\sigma^2(S-t)}{\sigma\sqrt{S-t}} \tag{3.29}$$

where the displacement is $0 \le \delta \le \frac{1}{\tau_i}$ [5]. Moreover, the assumption is made that there exists a real valued δ for which $F(t,S,T)+\delta > 0$ for all $i \in \{0,1,\ldots,N-1\}$. We define the displaced forward rate, $\tilde{F}(t,S,T)$ as

$$\tilde{F}(t,S,T) = F(t,S,T) + \delta. \tag{3.30}$$

The Brace Gątarek Musiela model also does not allow negative rates and will be discussed in the next section.

3.3. Brace Gatarek Musiela (BGM) model

In this section, a short description of the used BGM model is given.

In the BGM model, the forward rates are modelled and not the short-rate as in the Hull-White model. For each expiry date, T_i, the forward rate, $F(t,T_i,T_{i+1})$, is modelled with individual dynamic. Recall that the forward rate is defined in equation (2.25). The BGM model follows a log-normal distribution. Therefore, the forward rate volatilities can be found

using Black's formula for caps and floors. Since a log-normal process does not allow for negative rates, displaced forward rates, $\tilde{F}(t,S,T)$, are used, defined in equation (3.30). In this thesis, a 1-factor BGM model is used, according to [32]. Herein, the (displaced) forward rate dynamics are given by

$$\mathrm{d}F(t,T_i,T_{i+1}) = \mathrm{d}\tilde{F}(t,T_i,T_{i+1}) = \tilde{F}(t,T_i,T_{i+1})\sigma_{bgm}(T_i)\mathrm{d}W^{T_{i+1}}(t) \qquad t\in[0,T_i] \tag{3.31}$$

where the drift is set to 0 and $\sigma_{bgm}(T_i)$ is the (relative, instantaneous) volatility for expiry date T_i and chosen to be constant. The forward rates have initial conditions $\tilde{F}(t_0,T_i,T_{i+1})$.

Note that each forward rate has a Brownian motion under its own measure, T_{i+1}-measure. A homogeneous measure is introduced to simplify the simulation, namely the spot measure, $\mathbb{Q}^{T_{q(t)}}$ with $q(t)$ defined as an integer for which $T_{q(t)-1} \le t < T_{q(t)}$ holds. The spot-measure has $N(t)$ as numéraire, which is defined with $N(t_0)=1$ and, for T_i with $i\in\{0,1,\ldots,N-1\}$, by

$$\begin{aligned} N(T_i) &= \prod_{j=0}^{i-1}\frac{1}{P(T_j,T_{j+1})} \\ &= \prod_{j=0}^{i-1}(1+\tau_i F(T_j,T_j,T_{j+1})). \end{aligned} \tag{3.32}$$

where the definition of the forward rate is used, equation (2.25). Moreover, to understand the formulation of $N(t)$ consider the following process: at time $T_0=0$ one euro is invested in a zero-coupon bond maturing at time T_1. Then, at time T_1, the obtained money is

$$\frac{1}{P(T_0,T_1)} = 1+\tau_0 F(T_0,T_0,T_1) \tag{3.33}$$

This amount is reinvested in the zero-coupon bond maturing at time T_2 and the value of the portfolio is

$$\frac{1}{P(T_0,T_1)}\frac{1}{P(T_1,T_2)} = (1+\tau_0 F(T_0,T_0,T_1))(1+\tau_1 F(T_1,T_1,T_2)) \tag{3.34}$$

Continuing this process until time T_{N-1}.

To change from the T_{i+1}-measure to the spot-measure, $\mathbb{Q}^{T_{q(t)}}$, we first show the transition from the T_{i+1}-measure to the T_i-measure. Hence, $P(t,T_i)$ can be written as

$$\begin{aligned} P(t,T_i) &= P(t,T_{q(t)})\prod_{j=q(t)}^{i-1}\frac{P(t,T_{j+1})}{P(t,T_j)} \\ &= P(t,T_{q(t)})\prod_{j=q(t)}^{i-1}\frac{1}{\left(1+\tau_j F(t,T_j,T_{j+1})\right)} \end{aligned} \tag{3.35}$$

Using equation (3.35), the Radon-Nikodym derivative to change from the T_{i+1}-measure to the spot measure T_{i+1}-measure is given by

$$\lambda^i_{i+1}(t) = \left.\frac{\mathrm{d}\mathbb{Q}^{T_i}}{\mathrm{d}\mathbb{Q}^{T_{i+1}}}\right|_{\mathcal{F}(t_0)} = \frac{P(t,T_i)/P(t_0,T_i)}{P(t,T_{i+1})/P(t_0,T_{i+1})} = (1+\tau_i F(t,T_i,T_{i+1}))\frac{P(t_0,T_{i+1})}{P(t_0,T_i)} \tag{3.36}$$

From which follows

$$\begin{aligned} \mathrm{d}\lambda^i_{i+1}(t) &= \frac{P(t_0,T_{i+1})}{P(t_0,T_i)}\tau_i \mathrm{d}F(t,T_i,T_{i+1}) \\ &= \frac{P(t_0,T_{i+1})}{P(t_0,T_i)}\tau_i \tilde{F}(t,T_i,T_{i+1})\sigma_{bgm}(T_i)\mathrm{d}W^{T_{i+1}}(t) \end{aligned} \tag{3.37}$$

where equation (3.31) is used. Hereafter, dividing by $\lambda^i_{i+1}(t)$ gives

$$\frac{\mathrm{d}\lambda^i_{i+1}(t)}{\lambda^i_{i+1}(t)} = \frac{\tau_i \tilde{F}(t,T_i,T_{i+1})\sigma_{bgm}(T_i)}{1+\tau_i F(t,T_i,T_{i+1})}\mathrm{d}W^{T_{i+1}}(t) \tag{3.38}$$

Now, using Girsanov theorem, we obtain

$$\mathrm{d}W^{T_{i+1}}(t) = \mathrm{d}W^{T_i}(t) + \frac{\tau_i \tilde{F}(t,T_i,T_{i+1})\sigma_{bgm}(T_i)}{1+\tau_i F(t,T_i,T_{i+1})}\mathrm{d}t \tag{3.39}$$

Moreover, when applying this multiple times, one obtains

$$\begin{aligned}
\mathrm{d}W^{T_{i+1}}(t) &= \mathrm{d}W^{T_i}(t) + \frac{\tau_i \tilde{F}(t,T_i,T_{i+1})\sigma_{bgm}(T_i)}{1+\tau_i F(t,T_i,T_{i+1})}\mathrm{d}t \\
&= \mathrm{d}W^{T_{i-1}}(t) + \left(\frac{\tau_i \tilde{F}(t,T_i,T_{i+1})\sigma_{bgm}(T_i)}{1+\tau_i F(t,T_i,T_{i+1})} + \frac{\tau_{i-1} \tilde{F}(t,T_{i-1},T_i)\sigma_{i-1}}{1+\tau_{i-1} F(t,T_{i-1},T_i)}\right)\mathrm{d}t \\
&\vdots \\
&= \mathrm{d}W^{T_{q(t)}}(t) + \sum_{j=q(t)}^{i} \frac{\tau_j \tilde{F}(t,T_j,T_{j+1})\sigma_{bgm}(T_j)}{1+\tau_j F(t,T_j,T_{j+1})}\mathrm{d}t
\end{aligned} \tag{3.40}$$

Therefore, the dynamics of $\tilde{F}(t,S,T)$ under the $\mathbb{Q}^{T_{q(t)}}$-measure become

$$\frac{\mathrm{d}\tilde{F}(t,T_i,T_{i+1})}{\tilde{F}(t,T_i,T_{i+1})} = \sigma_{bgm}(T_i)\sum_{j=q(t)}^{i} \frac{\tau_j \tilde{F}(t,T_j,T_{j+1})\sigma_{bgm}(T_j)}{1+\tau_j F(t,T_j,T_{j+1})}\mathrm{d}t + \sigma_{bgm}(T_i)\mathrm{d}W^{T_{q(t)}}(t) \qquad t\in[0,T_i] \tag{3.41}$$

The solution for the SDE is given with Ito's lemma by

$$\tilde{F}(t,T_i,T_{i+1}) = \tilde{F}(t_0,T_i,T_{i+1})\exp\left(\int_{t_0}^{t}\sigma_{bgm}(T_i)\mathrm{d}W^{\mathbb{Q}^{spot}}(s) + \int_{t_0}^{t}\left(\sigma_{bgm}(T_i)\sum_{j=q(s)}^{i}\frac{\tau_j \tilde{F}(s,T_j,T_{j+1})\sigma_{bgm}(T_j)}{1+\tau_j F(s,T_j,T_{j+1})} - \frac{1}{2}\sigma_{bgm}(T_i)^2\right)\mathrm{d}s\right) \tag{3.42}$$

3.3.1. Interpolation of the discount factors

The zero-coupon bond for the expiry date, T_{i+1}, is given by

$$P(T_0,T_{i+1}) = \prod_{j=0}^{i}\frac{1}{1+\tau_n F(T_j,T_j,T_{j+1})} \tag{3.43}$$

However, for non-expiry dates, an interpolation technique is needed. The author of [32] compared different interpolation techniques and introduced a technique in which the forward rates are interpolated and for which a zero-coupon bond at time t with maturity T is given by

$$P(t,T) = \frac{1+(T_{q(T)}-T)\left(f_T\tilde{F}(t,T_{q(T)-1},T_{q(T)})-\delta\right)}{1+(T_{q(t)}-t)\left(f_t\tilde{F}(t,T_{q(t)-1},T_{q(t)})-\delta\right)}\left(\prod_{i=q(t)}^{q(T)-1}\frac{1}{1+\tau_i F(t,T_i,T_{i+1})}\right) \tag{3.44}$$

with

$$f_t = \frac{\tilde{F}(t_0,t,T_{q(t)})}{\tilde{F}(t_0,T_{q(t)-1},T_{q(t)})} \tag{3.45}$$

4

Simulation and calibration

This chapter will discuss the simulation and calibration of both the Hull-White model and the BGM model. For the Hull-White model, the volatility function, $\sigma_{hw}(t)$, needs to be calibrated. For the BGM model, each forward rate, F_i, has a constant volatility, $\sigma_{bgm}(T_i)$. In [29], a complete overview of different volatility and calibration structures is given. For ease of implementation, it is chosen to use constant volatility for each forward rate.

First, the simulation of both models will be discussed. After which, we will discuss which calibration instrument will be used for both models and explain the calibration for both models. Finally, this chapter concludes with the difference between a single and multi-curve framework.

4.1. Monte Carlo simulation

In this thesis, Monte Carlo simulation is used for simulation of the Hull-White dynamics, equation (3.20), and the BGM dynamics, equation (3.41), which both depend on a random process, the Brownian process. Therefore, a large number of paths are generated for the short-rate (or forward rate) to reach a broad set of possible outcomes. The advantage of Monte Carlo simulation is that it is easy to implement and an intuitive technique. To create the random paths, first, standard normal random numbers are drawn for each path and each time point[1]. The convergence of the Monte Carlo simulated is given by one divided by the square root of the number of paths used in the simulation [26]. The next step is to choose the type of discretisation of the integral.

One approach of discretisation is Euler's discretisation which is based on the left rectangle rule for an uniform partition $a = x_1 < \cdots < x_N = b$ with $x_i - x_{i-1} = \Delta$:

$$\int_a^b f(x)\mathrm{d}x = \lim_{\Delta \to 0} \sum_{x=a}^{b} f(x_i)\Delta \tag{4.1}$$

For a stochastic derivative, $S(t)$, with drift $m(t)$ and diffusion $\sigma(t)$, and dynamics

$$\mathrm{d}S(t) = m(t)\mathrm{d}t + \sigma(t)\mathrm{d}W(t) \tag{4.2}$$

the Euler discretisation for each next (constant) time step of size Δ is given by

$$S(t+\Delta) = S(t) + m(t)\Delta + \sigma(t)\sqrt{\Delta}Z \tag{4.3}$$

where Z has a standard normal distribution, $\mathcal{N}(0,1)$. For an Euler discretisation, the local error is equal to the square of the step size.

Another approach is that of an exact solution of the integration (of equation (4.2), which avoids the error that is caused by the step size in Euler's discretisation. The exact solution is given by integration and using the property, $aZ + b \sim \mathcal{N}(b, a^2)$, of the normal distribution of Z, such that :

$$S(t+\Delta) = S(t) + \int_t^{t+\Delta} m(s)\mathrm{d}s + \sqrt{\int_t^{t+\Delta} \sigma^2(s)\mathrm{d}s} \cdot Z \tag{4.4}$$

When $m(t)$ and $\sigma(t)$ are independent of $S(t)$, the integral can be calculated analytically. However, when they do contain $S(t)$ this is not possible and Euler's discretisation should be chosen.

[1] Standard normal random numbers are generated with `numpy.random.normal`.

4.1.1. Hull-White simulation

For the simulation of the interest-rate, $r(t)$, the exact solution is used. In equation (3.20), the dynamics of $r(t)$ are given. Note that in the dynamics of $r(t)$, $\mathrm{d}r(t)$, do not depend on $r(t)$. Therefore, the equation (3.22) is rewritten using the property, $aZ+b \sim \mathcal{N}(b, a^2)$, of the standard normal distribution Z, such that the integrals over the time interval $[t_k, t_{k+1}]$ are given by

$$r(t_{k+1}) = r(t_k) + \int_t^{t_{k+1}} \theta(s)\mathrm{d}s + \sqrt{\int_{t_k}^{t_{k+1}} \sigma_{hw}^2(s)\mathrm{d}s} \cdot Z \tag{4.5}$$

In this thesis, $\sigma_{hw}(s)$ is chosen to be piecewise-constant with $\sigma_{hw}(T_{i-1})$ constant in the interval of maturities, $[T_j, T_{j+1})$. Therefore, the time steps are chosen such that the maturity dates T_j are exactly on one of the simulated times. For $\sigma_{hw}(s) \in [t_k, t_{k+1}]$ the variance can be written as:

$$\int_{t_k}^{t_{k+1}} \sigma_{hw}^2(s)\mathrm{d}s = \sigma_{hw}^2(t_k)\left(t_{k+1} - t_k\right) \tag{4.6}$$

Furthermore, the integral in the drift term is given by

$$\begin{aligned}
\int_{t_k}^{t_{k+1}} \theta(s)\mathrm{d}s &= \int_{t_k}^{t_{k+1}} \frac{\partial f^r(0,s)}{\partial s}\mathrm{d}s + \int_{t_k}^{t_{k+1}} \int_{t_0}^{s} \sigma^2(u)\mathrm{d}u\mathrm{d}s \\
&= f^r(0,t_{k+1}) - f^r(0,t_k) + \int_{t_k}^{t_{k+1}} \left(\int_{t_k}^{s} \sigma^2(u)\mathrm{d}u + \int_{t_0}^{t_k} \sigma^2(u)\mathrm{d}u \right)\mathrm{d}s \\
&= f^r(0,t_{k+1}) - f^r(0,t_k) + \frac{1}{2}(t_{k+1}-t_k)^2\sigma_{hw}(t_k)^2 + (t_{k+1}-t_k)\sum_{j=0}^{k-1} \sigma_{hw}(t_j)^2(t_{j+1}-t_j)
\end{aligned} \tag{4.7}$$

where in the last line the fact that the volatilities are piece-wise constant is used. An exact solution for the money-market account and zero-coupon bond simulation are found in a similar manner and can be found in Appendix B.2 and the simulation including the mean-reversion parameter in Appendix B.1.

4.1.2. BGM simulation

In equation (3.42) the exact solution for the forward rate dynamics are given. Since there is no analytic solution for the drift term due to terms of $\tilde{F}(s, T_j, T_{j+1})$, $F(s, T_j, T_{j+1})$, it chosen to use Euler's discretisation. The discretisation for each time step from t_k to t_{k+1} is given by

$$\tilde{F}(t_{k+1}, T_i, T_{i+1}) = \tilde{F}(t_k, T_i, T_{i+1}) e^{\sigma_{bgm}(T_i)\sqrt{t_{k+1}-t_k}Z + \left(\sigma_{bgm}(T_i)\sum_{j=q(t_k)}^{i} \frac{\tau_j \tilde{F}(t_k,T_j,T_{j+1})\sigma_{bgm}(T_j)}{1+\tau_j F(t_k,T_j,T_{j+1})} - \frac{1}{2}(\sigma_{bgm}(T_i))^2\right)(t_{k+1}-t_k)} \tag{4.8}$$

4.2. Calibration

The Hull-White model and BGM model are generally calibrated to financial interest rate derivatives that are liquid in the market: caps, floors or swaptions. The choice of calibration may depend on the products that are simulated, on the available data or the computation time. Since this thesis compares the Hull-White model against the BGM model, we want to calibrate to the same market instrument.

When calibrating to cap or floors a set of maturity dates, T_i, is chosen with $T_i \in \{T_1, \ldots, T_n\}$. For the Hull-White model, for each period, a volatility can be found; equation (4.14). For the BGM model, the caplet/floorlet volatilities of each period can directly be used as constant volatility for each corresponding forward rate; equation (4.16). When calibrating to swaptions, a set of swaptions need to be chosen with different swaption maturities, T_i, and the swap tenor, swap length, is given by T_n. Where the T_i can be used to bootstrap the Hull-White volatilities and T_n is to be chosen, see Appendix C.3. For the BGM model, the swap rate volatility can be approximated with a weighted sum of BGM volatilities, see equation (5.10), which can be used to find the BGM volatilities. The swap tenors are often chosen with the co-terminal property, where all swap tenors are chosen such that all swaps end on the same date. The co-terminal depends on the portfolio that needs to be simulated. For example, if the portfolio only exists out of one 5 year swap, the co-terminal is given in Table 4.1.

swaption expiry (T_i)	swap tenor (T_n)
1	4
2	3
3	2
4	1

Table 4.1: Co-terminal for the calibration of a 5 year swap with T_i the swaption expiry and T_n the swap tenor

For the BGM model, calibrating to caplets has a high preference for a short calibration time, as these volatilities can directly be used in the forward rate dynamics. However, if only one swap is to be priced and the swaption data corresponding with this swap is available, one does not need to calibrate to caplets and can determine the EPE from this swaption data. Nonetheless, the research question is to simulate a whole portfolio. The calibration to swaption brings a new problem: which co-terminals to choose if the maturities of the swap in the portfolio differ. Since the calibration to swaptions is not guaranteed to be more accurate than caplets for each portfolio, it is chosen to calibrate to caplets. Another advantage of caplets is that the calibration instruments do not need adjustments every time a new instrument is added to the portfolio.

4.2.1. Hull-White calibration

The caplets used for calibration have fixing dates $T_i \in \{T_1, \ldots, T_n\}$ and an at-the-money strike price K. For the calibration, first, the mean-reversion parameter, α, is chosen, after which we will calibrate the time-dependent volatility. Recall that the mean-reversion parameter, α, is chosen to be zero.

The volatility, $\sigma_{hw}(t)$, is simplified to a piecewise-constant volatility, $\sigma_{hw}(T_{i-1})$, for which, for each expiry $0 < T_1 < \cdots < T_n$ a constant $\sigma_{hw}(T_{i-1})$ will be found for interval $[T_{i-1}, T_i)$, see Figure 4.1.

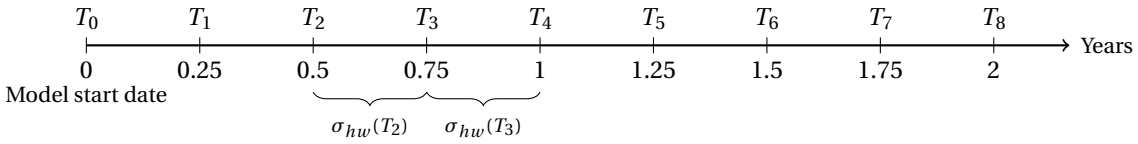

Figure 4.1: Piecewise-constant volatility grid with $\Delta = 0.25$ years

The piecewise constant volatility for the Hull-White model can be found by local optimisation (bootstrapping) or by global optimisation. In bootstrapping, each next volatility term is based on all the previously-found volatilities. In global optimisation, all the volatility terms are optimised at the same time.

Local optimisation Local optimisation can be done by bootstrapping the Hull-White volatilities to the market-implied caplet volatilities. Moreover, the fact that a caplet payoff can be written as a put on a zero-coupon bond is used. For a detailed description of the calibration with all calculations, we refer to Appendix C.1. In short, for expiry time T_i and $\tau_i = T_{i+1} - T_i$ (adjusted to the day count convention), the caplet payoff can be written as

$$V_i^{\text{cpl}}(t, T_i, T_{i+1}) = N(1+\tau_i K)P(t,T_i)\mathrm{E}^{T_i}\left[\max\left(\frac{1}{1+\tau_i K} - P(T_i, T_{i+1}), 0\right)\middle|\mathscr{F}_t\right] \tag{4.9}$$

It follows that

$$V_i^{\text{cpl}}(t, T_i, T_{i+1}) = (1+\tau_i K)V_p^{\text{zcb}}(t, T_i, T_{i+1}, \frac{1}{1+\tau_i K}) \tag{4.10}$$

$$V_p^{\text{zcb}}(t, T_i, T_{i+1}, X) = NP(t,T_i)\left(X\Phi(-d_-^{\text{zcb}}) - P(t,T_i,T_{i+1})\Phi(-d_+^{\text{zcb}})\right) \tag{4.11}$$

$$d_\pm^{\text{zcb}} = \frac{\ln(\frac{P(t,T_i,T_{i+1})}{X}) \pm \frac{1}{2}\text{Var}[P(T_i,T_{i+1})|\mathscr{F}_t]}{\sqrt{\text{Var}[P(T_i,T_{i+1})|\mathscr{F}_t]}} \tag{4.12}$$

Now, to find the volatilities for the Hull-White model, first, the caplet price is calculated, using the market-implied volatilities. This caplet price is used to find the variance of the zero-coupon bond, see equations (4.10)-(4.12). Hereafter, to find the Hull-White volatilities, $\sigma_{hw}(T_{i-1})$, each market zero-coupon bond variance is set equal to the zero-coupon bond variance under the Hull-White model.

Therefore, the objective function is stated as:

$$\text{Var}[P(t_0, T_i, T_{i+1}, \sigma_{hw}(T_{i-1}))] = \sigma_{mkt}^{\text{zcb}}(t_0, T_i, T_{i+1}, K)^2(T_i - t_0) \tag{4.13}$$

where the closed-form solution of the zero-coupon bond variance under the Hull-White model for zero-mean reversion is given in equation (3.26). From which Hull-White volatilities, $\sigma_{hw}(T_{i-1}, T_i)^2$, can be found and for zero-mean reversion are given by

$$\sigma_{hw}(T_{i-1})^2 = \frac{\frac{\sigma_{mkt}^{\text{zcb}}(t_0,T_i,T_{i+1},K)^2(T_i-t_0)}{(T_{i+1}-T_i)^2} - \sum_{k=1}^{i-1}\sigma_{hw}(T_{k-1})^2(T_k - T_{k-1})}{T_i - T_{i-1}} \tag{4.14}$$

The caplet volatility calibration for a Hull-White model with mean-reversion parameter is given in equation (C.7).

Global optimisation Another approach is optimising all the volatility terms at the same time, in a multi-variable global optimisation, where the Hull-White volatilities are optimise by comparing the implied caplet Hull-White volatilities with the market caplet volatilities for each expiry time (T_i).

$$\Omega(\sigma_{hw}(T_0),\dots,\sigma_{hw}(T_{n-1})) = \min \sum_{i=1}^{n} \left[\text{caplet vol market}(T_i) - \text{caplet vol hw}(T_i)\right]^2 \tag{4.15}$$

with the constraint that all the volatilities, $\sigma_{hw}(T_i)$, are positive. Moreover, one might consider multiplying the difference with a large number since the objective function works with many small numbers (<1) and a squared error.
For the Hull-White model, the volatility is given in equation (4.14). Moreover, both the local optimisation as the global optimisation will be compared. A recap of the Hull-White calibration process is shown in Figure 4.2.

Figure 4.2: Hull-White volatility calibration process to caplets for each bootstrapping step with reference to the equations for the given change

4.2.2. BGM calibration

The BGM calibration to caps uses the fact that the BGM model has a log-normal distribution and Black's formula (definition 2.2.8). Moreover, it is chosen to have a constant volatility for each forward rate and calibrate to ATM caplets. Now, using Black's formula for caplets one finds that the dynamics of a forward rate $F_i(t) := F(t,T_i,T_{i+1})$ the BGM volatility, $\sigma_{bgm}(T_i)$, is given by

$$\sigma_{bgm}(T_i) = \sigma^{\text{cpl}}_{mkt}(t_0,T_i,T_{i+1}) \tag{4.16}$$

where $\sigma^{\text{cpl}}_{mkt}(t_0,T_i,T_{i+1})$ is the market caplet volatility and described by Black's formula as an option on the forward rate $F(t,T_i,T_{i+1})$).

For the BGM model, the volatility is given in equation (4.16). A recap of the BGM calibration process is shown in Figure 4.3.

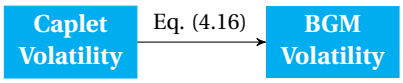

Figure 4.3: Caplet volatility can directly be used in the BGM model

4.3. Single-curve and multi-curve framework

The multi-curve framework has received more focus since the financial crisis in 2007/2008. Before this crisis, people may have underestimated counterparty risk, as people assumed banks were stable companies and governments were there to back them up. Therefore, the difference between, for example, the 3-months EURIBOR and 6-months EURIBOR were close to zero (or other reference rates). In the new setting, the risk of default needs to be incorporated, where longer tenor periods have higher risks. Consequently, a spread between the different yield curves arose [3]. Henceforth, we introduce a multi-curve framework to include both the discounting yield curve, $P^d(t,T)$, and the multiple forecasting yield curves, $P^{f_i}(t,T)$, for each tenor structure, often 1-month, 3-months, 6-months and 12-months.

First, we explain how the yield curves are obtained from the market, after which we present how to implement the multi-curve framework.

The first step in obtaining the discounting curve (and similarly the forecasting curve) is stripping of the discount/forecast factors from some market instruments [1] (the discount/forecast factors are given as data input in our simulation). The discount factors are retrieved for each relevant date of the interest rate products in the portfolio. Then, the second step is to interpolate these discount factors to obtain a continuous function for all time points. Remark that the Hull-White model uses a discounting/forecasting yield curve for the instantaneous forward rate in θ, see equation (3.9). Therefore, the yield curve should be twice differentiable and continuous. According to [16], a cubic spline interpolation contains these properties. Therefore, cubic spline interpolation is used to obtain a continuous curve. The forecasting curves are

only obtained for the relevant tensor structures, which correspond with the tenor structure of the derivatives in a portfolio.

The difference between a single-curve and multi-curve framework is that the discounting and forecasting curves are not the same. Moreover, in a multi-curve framework, one wants to obtain the discount factors and forecast factors for future time points (through Monte Carlo simulation). To obtain multiple yield curves from the simulation, first, a single-curve simulation is performed, after which the other curves are obtained through the initial spreads between the curves [25], [34]. The spread, at time 0 with maturity T, between the simulated discount/forecast factor, $P^A(t,T)$, and another factor, $P^B(t,T)$ (e.g. $B = \{d, 1M, 3M, 6M, 12M\}/A$), is given by

$$P_s(0,T) = \frac{P^B_{mkt}(0,T)}{P^A_{mkt}(0,T)}. \tag{4.17}$$

Moreover, the assumption is made that the spreads between the initial curve, $P^A(t,T)$, and derived curves, $P^B(t,T)$, are deterministic and not changed with time. Now, the discount/forecast factors, $P^B(t,T)$, for a future time point t can be derived by:

$$P^B_{hw}(t,T) = P^A_{hw}(t,T)P_s(0,T) = P^A_{hw}(t,T)\frac{P^B_{mkt}(0,T)}{P^A_{mkt}(0,T)} \tag{4.18}$$

Under the risk-neutral measure with numéraire, $M(t)$, the zero-coupon-bond over numéraire values is a martingale and, thus, the simulated discount/forecast factors at time 0 are equal to the initial market discount/forecast factors, the following holds:

$$\mathbb{E}\left[\frac{M(0)}{M(t)}P^A_{hw}(t,T)\middle|\mathscr{F}_0\right] = P^A_{hw}(0,T) = P^A_{mkt}(0,T) \tag{4.19}$$

Now, using this equation, the expectation of the derived discount/forecast factors is given by

$$\mathbb{E}\left[\frac{1}{M(t)}P^B_{hw}(t,T)\right] = \mathbb{E}\left[\frac{1}{M(t)}P^A_{hw}(t,T)\frac{P^B_{mkt}(0,T)}{P^A_{mkt}(0,T)}\right] = P^B_{mkt}(0,T) \tag{4.20}$$

resulting in a simulated discount/forecast factors, $P^A_{hw}(t,T)$, and a way to derive other factors, $P^B_{mkt}(t,T)$ for multiple paths and time points. For example, let the simulated factors be the 3-months forecasting, $P^{3m}_{hw}(t,T)$, and the factors one wants to obtain be the discount factors, $P^d_{hw}(t,T)$, and the 6-month forecasting factors, $P^{6m}_{hw}(t,T)$. These are then given by

$$P^d_{hw}(t,T) = P^{3m}_{hw}(t,T)\frac{P^d_{mkt}(0,T)}{P^{3m}_{mkt}(0,T)} \tag{4.21}$$

and

$$P^{6m}_{hw}(t,T) = P^{3m}_{hw}(t,T)\frac{P^{6m}_{mkt}(0,T)}{P^{3m}_{mkt}(0,T)}. \tag{4.22}$$

Furthermore, to determine which curve to simulate, consider the Hull-White model calibration to a zero-coupon bond put value using a discounting curve, $P^d(0,t)$, and a forecasting curve, $P^{f_j}(0,t)$. Next, equation (4.9) is rewritten considering both curves, shown in Appendix D. Since we can rewrite this equation to only the forecasting curve, $P^{f_j}(0,t)$, calibrating to the forecasting curve is a logical choice. Moreover, for the BGM model, the forward rate is simulated for which forward factors are used. Therefore, it is chosen to use the forecasting curve as input.

These equations give a similar setting for the calibration as in the single curve framework, only now the model is calibrated using the forecasting curve, $P^{f_j}_{mkt}(0,T)$. Therefore, it is chosen to simulate the forecasting curve, $P^{f_j}_{hw}(0,T)$, in the single-curve simulation. Consequently, the forecasting curve is an input for the instantaneous forward rate used in $\theta(t)$.

For the BGM model, forwards with different tenor structures are needed to price swaps. First, the discount factors, $P^{f_j}_{bgm}(t,T)$, are calculated from which the corresponding forward rates, $F^{f_j}_i(t)$, can be found with the forward rate definition; equation (2.25).

Moreover, if a portfolio uses multiple forecasting curves, one needs to choose the forecasting curve for simulation, which curve is most used in a portfolio. The forecasting curve that is used as input for the simulation is chosen with Algorithm 1

Algorithm 1 How to choose simulation curve

```
sum = {}
for ti in tenorlist do
    sum[ti] = 0
    for swap in swaplist do
        if floatingtenor is ti then
            sum[ti] = sum[ti] + remaining swap duration × swap notional
        end if
    end for
end for
simulationtenor = max(sum.items(), key=lambda x: x[1])[0]
```

A recap of the single-curve and multi-curve simulation process for the Hull-White model and BGM model is shown in Figures 4.4, 4.5.

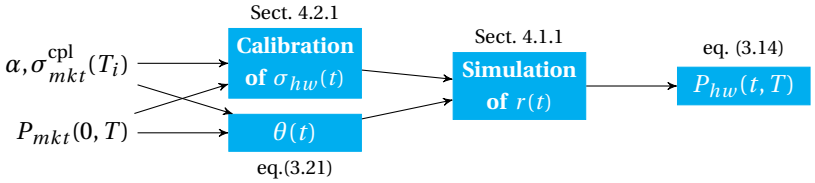

(a) Single-curve framework Hull-White

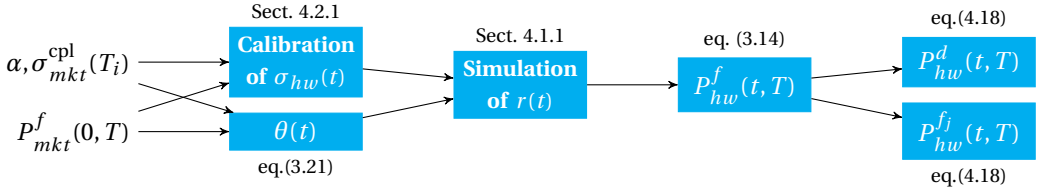

(b) Multi-curve framwork Hull-White

Figure 4.4: The different simulation structures and inputs for single and multi-curve Hull-White Monte Carlo simulation. The Hull-White single-curve framework has as input a initial yield curve, $P_{mkt}(0,T)$, a mean-reversion parameter α and market caplet volatilities $\sigma^{cpl}_{mkt}(T_i)$. Hereafter, Hull-White model volatilities $\sigma_{hw}(t)$, Hull-White model long-term mean $\theta(t)$ are calibrated and the Monte Carlo simulation of the short-rate, $r(t)$, is done. One yield curve is obtained from this short-rate for future time points, $P_{hw}(t,T)$. The difference with the multi-curve framework is that a certain forecasting curve is used as input, $P^f_{mkt}(0,T)$ with f either 1M, 3M, 6M or 12M, and multiple yield curves are obtained for future time points, $P^d_{hw}(t,T)$, $P^{f_j}_{hw}(t,T)$ with $f_j \in \{1M, 3M, 6M \text{ or } 12M\} \setminus f$

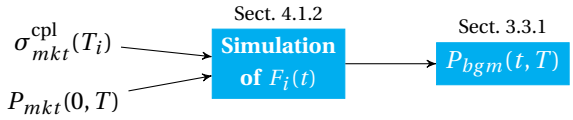

(a) Single-curve framework BGM

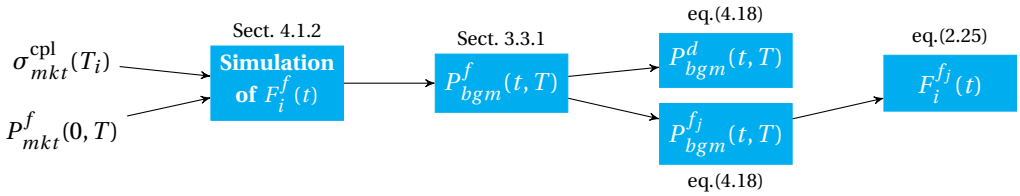

(b) Multi-curve framwork BGM

Figure 4.5: The different simulation structures and inputs for single and multi-curve BGM Monte Carlo simulation. The BGM single-curve framework has as input one initial yield curve, $P_{mkt}(0,T)$ and market caplet volatilities $\sigma^{\text{cpl}}_{mkt}(T_i)$. Hereafter, the Monte Carlo simulation of the forward rates, $F_i(t)$, is done. From this forward rates one yield curve is obtained for future time points, $P_{bgm}(t,T)$. The difference with the multi-curve framework is that a certain forecasting curve is used as input, $P^f_{mkt}(0,T)$ with f either 1M, 3M, 6M or 12M. Therefore, a forward rate $F^f_i(t)$ is simulated with tenor structure f. Hereafter, multiple yield curves are obtained for future time points, $P^d_{bgm}(t,T)$, $P^{f_j}_{bgm}(t,T)$ with $f_j \in \{1M, 3M, 6M \text{ or } 12M\} \setminus f$. Last, with these forecast factors, $P^{f_j}_{bgm}(t,T)$, the forward rate with different tenor structures can be found.

5

Validation of the results

In this chapter, a validation of the results of the Hull-White model and BGM model is discussed. First, the local and the global calibration of the Hull-White model are compared. Then, the validation of the calibration of both models is given, where we will compare the simulated caplet volatilities and discounting/forecasting curves against market data. Last, we provide a validation of the EPE and MTM of several single swaps. In the validation, we will consider different scenarios with single curve and multi-curve and different accrual periods. Moreover, it is chosen to provide a relevant number of different scenarios. However, not all scenarios will be shown, as in some cases, many combinations are possible, which will not enhance the validation. In the validation, the simulated caplet volatilities will be checked against the market volatilities. For the comparison, we will use a confidence interval of 95 %.

5.1. Hull-White model calibration methods

The calibration for the Hull-White model is chosen to have a time-dependent volatility and no mean-reversion. The calibration of the Hull-White model is described in section 4.2. In this section, local and global calibration methods are described. The results of the both methods are displayed in Figure 5.1.

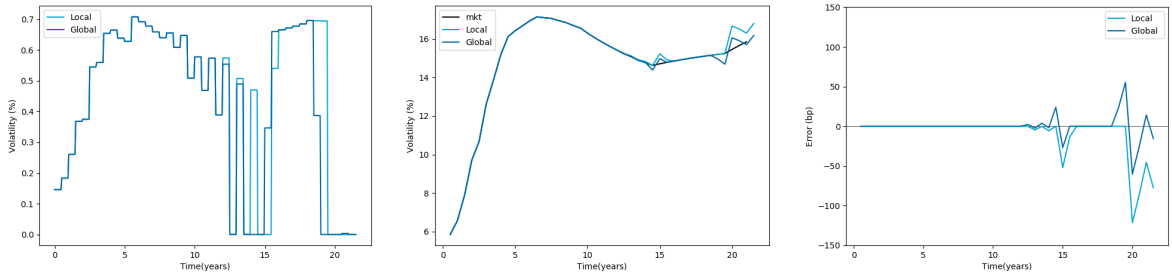

(a) Hull-White model volatility (b) Implied caplet volatility (c) Caplet implied volatility error

Figure 5.1: Volatility of the local and global calibration of the Hull-White model. (a) Calibrated Hull-White model volatility. (b) Analytically calculated caplet volatility from model volatility compared with market caplet volatility. (c) Error between analytically calculated caplet volatility and market in basis points (bp).

Recall that in finding the Hull-White volatility, $\sigma_{hw}(t)$, one first finds the Hull-White variance, $\sigma^2_{hw}(t)$, given in equation (4.14). During the local calibration, this value sometimes occurs to be negative. Therefore, if the exact calibrated value of $\sigma^2_{hw}(t)$ is negative, we set $\sigma^2_{hw}(t)$ to zero (closest nonnegative value), see Figure 5.1 (a). Consequently, not all values are exactly calibrated. In Figure 5.1 (c), the implied error due to the fact that an exact calibration is not possible is shown. At the end of this section, we will explain why this effect occurs.

The computation time of the calibration of the three methods is shown in Table 5.1. Since the calibration time of the global calibration is quite large, we try to improve the optimisation and call this method "Local & Global". Now, instead of optimising the caplet volatility, we optimise to the zero-coupon bond volatility, which is the last step of the calibration, shown in Figure 4.2. The optimisation function now becomes:

$$\Omega(\sigma_{hw}(T_0),\ldots,\sigma_{hw}(T_{n-1})) = \min \sum_{i=1}^{n} \left[\sigma^{\text{zcb}}_{mkt}(t_0,T_i,T_{i+1},K)^2 (T_i - t_0) - (T_{i+1}-T_i)^2 \sum_{k=0}^{i-1} \sigma_{hw}(T_k)^2 \left(T_{k+1}-T_k\right) \right]^2 \tag{5.1}$$

with the constraint that all the volatilities, $\sigma_{hw}(T_i)$, are positive.

Table 5.1: The calibration time of the Hull-White volatilities. Taken the mean and standard division of 10 runs.

Method	Mean (seconds)	Standard deviation
Local	0.043	0.005
Global	30.4	1.24
Local & Global	3.57	0.35

The errors of the three methods are shown in Figure 5.1(c) and Table 5.2. The table shows that for the global optimisation compared with the local optimisation, the mean square error reduces by a factor of 3 and the computation time of the local optimisation increases by a factor of 85 compared to the "local&global" optimisation. Therefore, we recommend choosing the local calibration for a fast calibration and a global optimisation calibration for the most accurate calibration. In this thesis, we do not have a time limitation. Therefore, we choose to use the method with global optimisation, as this method has the smallest error.

Table 5.2: Implied volatility error of different calibration methods for the Hull-White volatilities. The volatilities are in percentages (%).

Model	Mean absolute error	Max absolute error	Mean squared error
Local	0.1055	1.256	6.89
Global	0.0703	0.636	2.19

To explain the effect where the optimal Hull-White variance becomes negative, recall equation (4.14). In this equation, the Hull-White volatility, σ_i for the period $[T_{i-1}, T_i)$ is found by comparing the market zero-coupon bond variance to the analytic Hull-White zero-coupon bond variance. The Hull-White zero-coupon bond variance is given by a sum of all previous Hull-White variance multiplied with $(T_{i+1} - T_i)^2$. When this sum gets larger than the zero-coupon bond market variance divided by $(T_{i+1} - T_i)^2$, the numerator becomes negative. The largest errors in implied Hull-White caplet volatility are around 15 and 20 years, Figure 5.1 (c), which could be explained by the forecasting curve, Figure 5.2. In this figure, around 15 and 20 years, the slope declines slower; similar to the points, the Hull-White variance becomes negative.

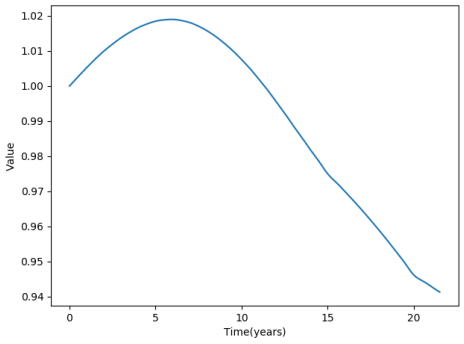

Figure 5.2: Plot of the forecasting curve

To substantiate this theory, we implement a parabolic forecasting curve, which is generated by

$$P(0,T) = \frac{-(T-6)^2}{1000} + 1.02 \tag{5.2}$$

and shown in Figure 5.3 (a). Equation (5.2) has its top at 6-years with a value of 1.02, similar to the forecasting curve. Figure 5.3 (b) shows the Hull-White volatilities generated with the market caplet volatilities and the parabolic forecasting curve. It shows that no negative volatilities occur. Figure 5.3 (c) shows the caplet market volatilities and implied Hull-White volatilities are the same. Figure 5.3 (d)-(f) shows what happens when 0.001 is subtracted from the forecast factor at a time of 10-years.

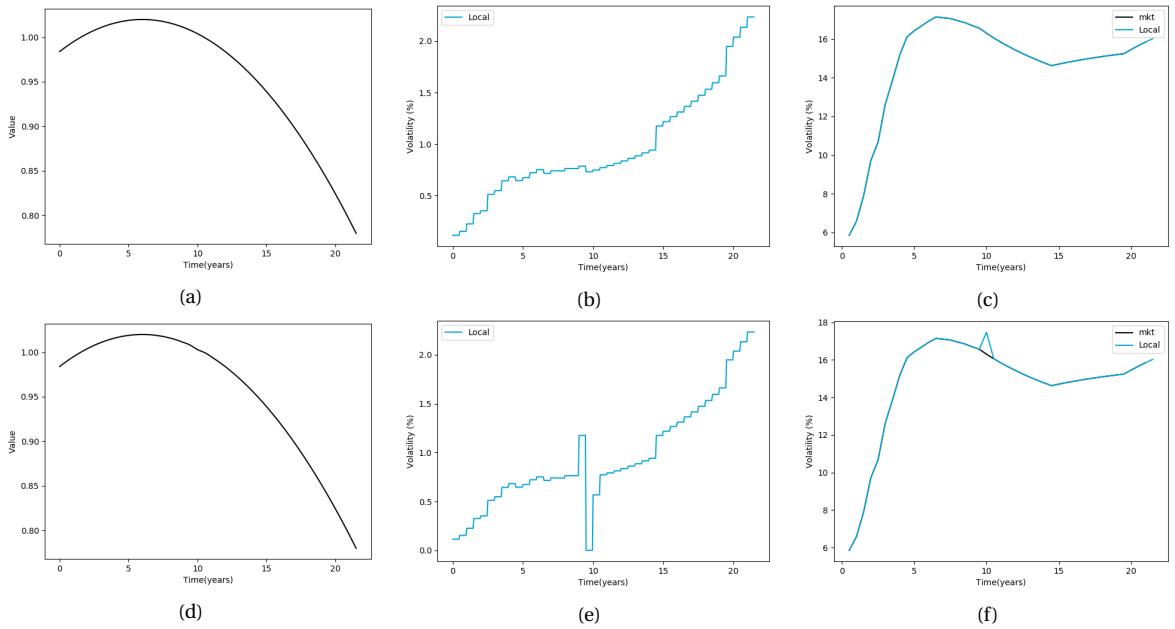

Figure 5.3: Plots of the effect of subtraction of 0.001 of the forecast factor at time 10-years. (a) parabolic curve described in equation (5.2). (b) Corresponding Hull-White volatilities. (c) The analytically calculated caplet volatility and market volatility. (d) The modified curve with subtraction of 0.001. (b) Corresponding Hull-White volatilities. (c) The analytically calculated caplet volatility and market volatility.

In Figure 5.3 (e), for the period from 9-years to 9.5-years, a higher Hull-White volatility occurs than in Figure (b) and from 9.5-years to 10-years a lower Hull-White volatility. When we investigate equation (4.14), for the higher period $T_{i-1} = 9$-years, $T_i = 9.5$-years, $T_{i+1} = 10$-years. Hence, for a lower value of $P(0, T_{i+1})$, this results in a higher zero-coupon bond put price, see equation (4.11). Therefore, a higher Hull-White volatility. For the period from 9.5-years to 10-years, the exact opposite happens, which results in a lower Hull-White volatility.

The inconsistencies that occur at 15-years and 20-years in the forecasting curve are caused by the retrieved data. The retrieved curve data for those points uses its own interpolation technique and data points, which are for us unknown.

5.1.1. Smoothing the curve

There are many available smoothing functions with which one can smooth a curve or set of points. Since this is out of the scope of our research question, we only give an example of the effect of a smoothing function. We will not provide an overview of different smoothing techniques nor an analysis on the effect of smoothing the curve. One of the smoothing functions is the Savitzky-Golay filter [31]. The filter can be applied to data points that are at an equal distance from each other. Now, for a given window, w, and degree r, it fits a polynomial of degree r, for each group of w consecutive points. The method generates a new set of points using these polynomials. A curve of 22 years with a 6-months accrual period has 44 points. Figure 5.4 shows the application of a Savitzky-Golay filter with a window of 23 and polynomials of degree 3. It shows that the calibration can now perfectly fit the market caplet volatilities.

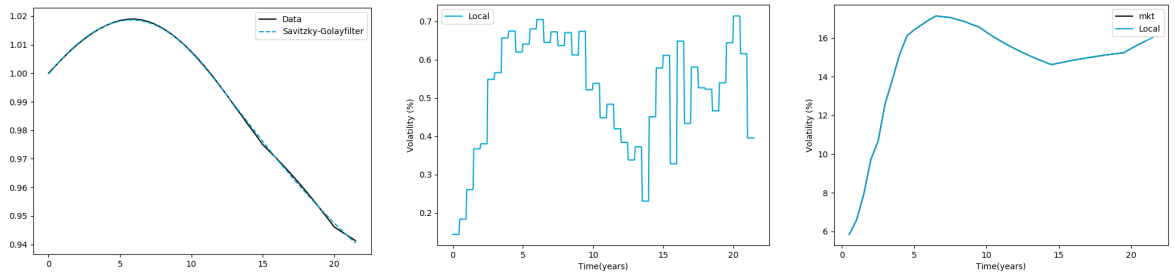

(a) Forecasting curve (b) Hull-White volatility (c) Caplet implied volatility

Figure 5.4: Plots of the application of the Savitzky-Golayfilter. (a) The market curve and the Savitzky-Golayfilter 6-months forecasting curve. (b) The Hull-White volatility. (c) The analytically calculated caplet volatility and market volatility.

5.2. Hull-White model and BGM model validation

The simulated Hull-White caplet volatilities (with global calibration) are compared with the market volatilities, shown in Figure 5.5. In Figure 5.5 (b), the errors with market caplet volatilities are shown, and in (c), the errors with the analytically implied volatilities (The implied caplet volatilities that are found using the Hull-White volatilities). The errors in Figure 5.5 (a)-(b) are because an exact calibration was not possible and not due to the simulation, as confirmed in (c). In Figure 5.5 (c), the market caplet volatilities are in between the confidence interval of the simulated volatilities.

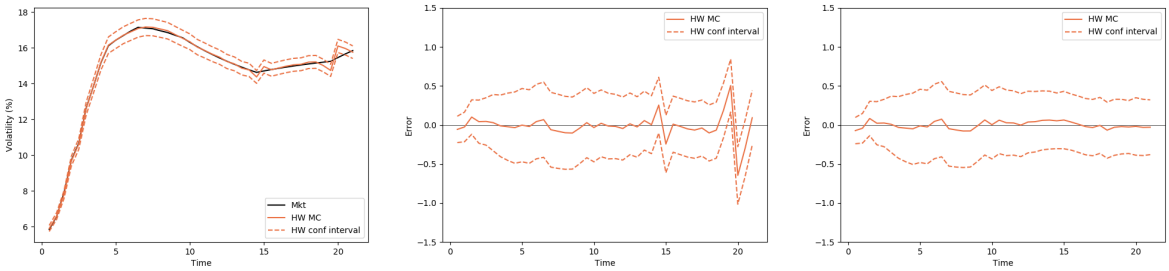

(a) Simulation of caplet volatilities (b) Error market caplet volatility (c) Error analytical caplet volatility

Figure 5.5: Plots of the simulated Hull-White caplet volatilities with 10000 paths. (a) The market caplet volatility and the the Hull-White simulation caplet volatility with a confidence interval of 95%. (b) The error between the simulated and market caplet volatility. (c) The error between the simulated and analytically implied caplet volatility. The analytically caplet volatility is implied by the Hull-White volatilities, which does not always have an exact solution.

For the BGM model, the caplet volatilities can be directly used as model volatilities, see equation (4.16). In Figure 5.6 (a), the simulated caplet volatilities and confidence interval of the BGM model are shown. In (b), the errors of the simulated and market caplet volatilities are given. The market volatilities are in the confidence interval of the simulated caplet volatilities.

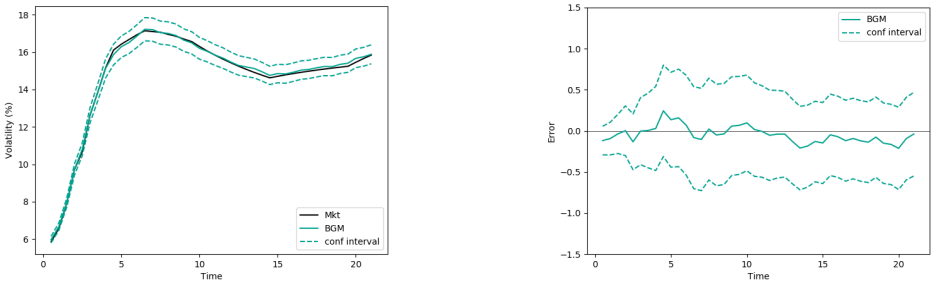

(a) Simulation of caplet volatilities (b) Error market caplet volatility

Figure 5.6: Plots of the BGM volatilities simulation with 10000 paths. (a) The market caplet volatility and the the BGM simulation caplet volatility with a confidence interval of 95%. (b) The error between the simulated and market caplet volatility.

5.3. Validation of the calibration to market curves

In this section, we will compare the simulated discount and forecast factors with the market input.

The simulated Hull-White forecast factors should be equal to the market forecast factors by equation

$$P^{f_j}_{\text{mkt}}(0,T) = \mathbb{E}\left[\frac{M(0)}{M(t)} P^{f_j}(t,T)\middle|\mathscr{F}_0\right] \tag{5.3}$$

with $M(t)$ the money account and $P^{f_j}(t,T)$ the simulated zero-coupon bond given in equation (3.14). Therefore, both forecast factors will be compared. The used forecast factors have a 6-months accrual period and will be either single or multi-curve. The forecast factors for time, t, 1, 5 and 15 years, are shown in Figure 5.7. The figure shows that Hull-White forecast factors are within the confidence interval. A multi-curve setting is used in Figure 5.7 (a) and (c) and a single-curve setting in (b).

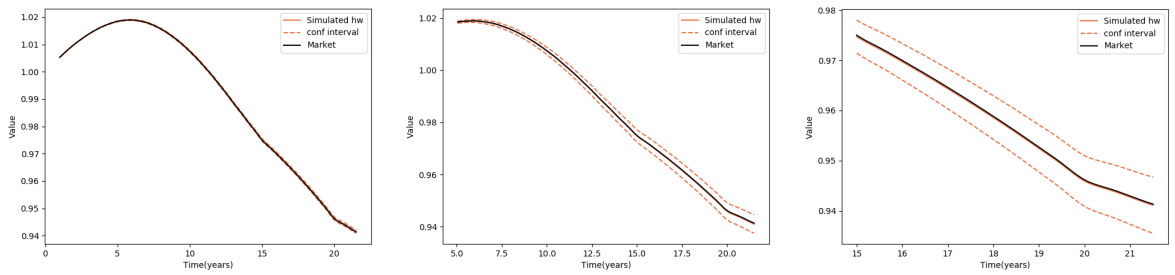

(a) (b) (c)

Figure 5.7: Plots of the market forecast factors and the simulated Hull-White forecast factors $P^{6m}(t,T)$ with a confidence interval of 95% and 10000 paths. (a) Multi curve with $t = 1Y$ and T varying. (b) Single curve with $t = 5Y$ and T varying. (c) Multi curve with $t = 15Y$ and T varying

For the discount factors, in the Hull-White model the money-market account $M(t)$ is given in equation (B.6) and for the BGM model the interpolated discount factors are given in equation (3.44). The relation between the market discount curve, $P^{\text{disc}}_{\text{mkt}}(0,t)$, and the money market account $M(t)$ is given by

$$P^{\text{disc}}_{\text{mkt}}(0,t) = \mathbb{E}\left[\frac{P^{\text{disc}}(t,t)}{M(t)}\middle|\mathcal{F}_0\right] = \mathbb{E}\left[\frac{1}{M(t)}\middle|\mathcal{F}_0\right] \tag{5.4}$$

The simulated discount factors are compared with the discount curve in Figure 5.8 and Figure 5.9. The figures show that for both models and scenarios the market curves are in the confidence interval of the model.

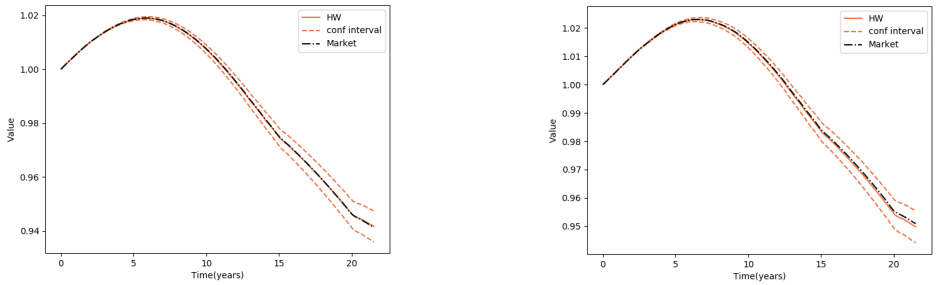

(a) Single Curve (b) Multi Curve

Figure 5.8: Plots of the market discount factors and the simulated Hull-White discount factors for different t with 10000 paths.

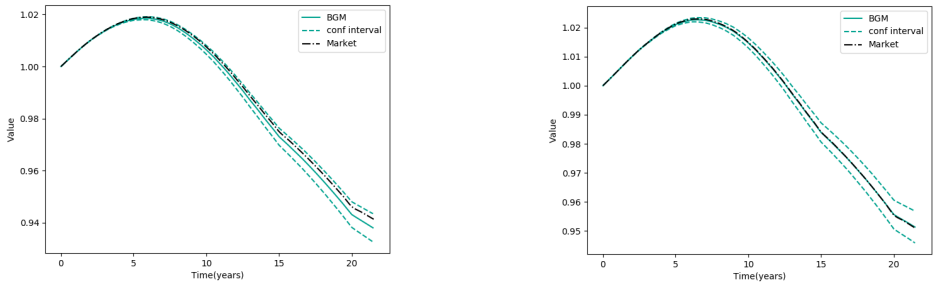

(a) Single Curve (b) Multi Curve

Figure 5.9: Plots of the market discount factors and the simulated BGM discount factors for different t with 10000 paths.

5.4. Validation EPE and MtM of a swap

The goal of this thesis is to compare both models on the Expected positive exposure (EPE) of a swap portfolio. To validate that they are calculated correctly, and the simulation is properly modelled, one can analytically calculate the Market-to-market (MTM) and estimate the EPE of a single swap and compare this with the results of the models.

To calculate the MTM of a swap (or swap portfolio), one uses the market curves for the discounting and the correct

forecasting factors. The MTM of both single, as multi-curve for different maturities and accrual periods are shown in Figure 5.10 and 5.11. The figures show that the MTM are in the confidence interval and thus validate that the model prices back to the market.

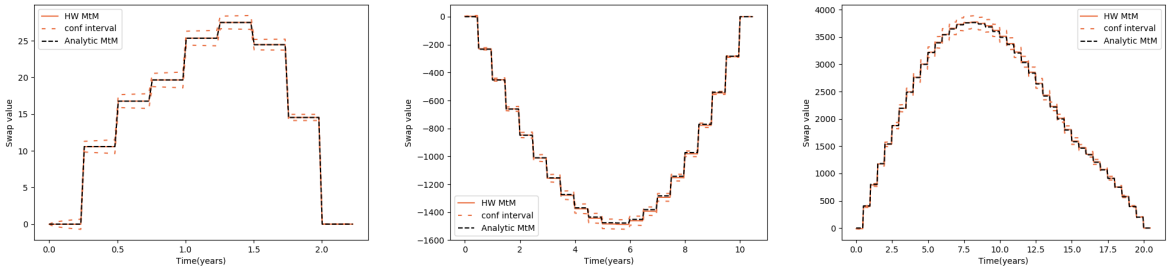

(a) (b) (c)

Figure 5.10: Plots of the analytic swap MTM and the simulated swap MTM of the Hull-White model and BGM model with 100000 paths. (a) 5-years payer swap with quarterly payments in a single curve framework. (b) 10-years receiver swap with semi-annual payments in a multi-curve framework. (c) 20-years payer swap with semi-annual payments in a single curve framework

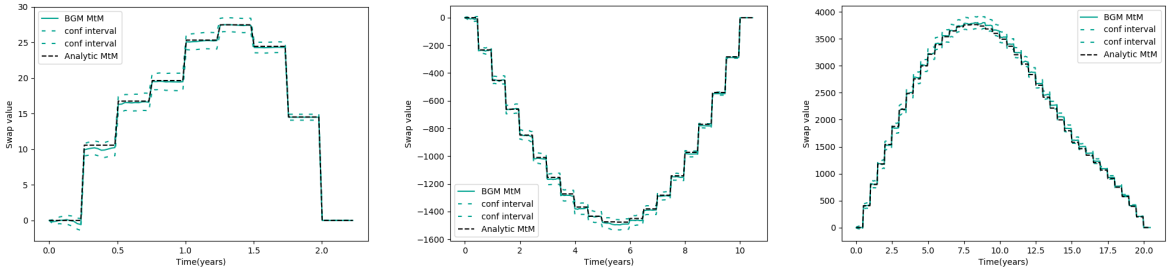

(a) (b) (c)

Figure 5.11: Plots of the analytic swap MTM and the simulated swap MTM of the Hull-White model and BGM model with 100000 paths. (a) 5-years payer swap with quarterly payments in a single curve framework. (b) 10-years receiver swap with semi-annual payments in a multi-curve framework. (c) 20-years receiver swap with semi-annual payments in a single curve framework

To estimate the EPE for the BGM model, an approximation of the swap rate volatility can be used [21]. In the paper, the swap rate volatility is expressed in terms of forward rate volatilities given the forward rate is log-normally distributed and the swap rate is approximately log-normally distributed [21]. As this is true for the BGM model, the (displaced) swap rate, $\tilde{S}_{i,n}(t)$, can be expressed by the sum of the weighted (displaced) forward rate [21]:

$$\tilde{S}_{i,n}(t) = \sum_{k=i}^{n} \omega_k(t)\tilde{F}(t, T_k, T_{k+1}) \tag{5.5}$$

with

$$\omega_k(t) = \frac{\tau_k P(t, T_{k+1})}{\sum_{k=i}^{n} \tau_k P(t, T_{k+1})} \tag{5.6}$$

The dynamics of a log-normal forward rate are given by

$$\mathrm{d}\tilde{F}(t, T_k, T_{k+1}) = \tilde{F}(t, T_k, T_{k+1})\tilde{\sigma}_k \mathrm{d}W(t) \tag{5.7}$$

Using the dynamics of $\tilde{F}_k$, it follows that

$$\sum_{k=i}^{n} \omega_k(t_0)\mathrm{d}\tilde{F}_k = \sum_{k=i}^{n} \omega_k(t_0)\tilde{F}(t, T_k, T_{k+1})\tilde{\sigma}_k \mathrm{d}W(t) \tag{5.8}$$

Therefore, the dynamics of the (displaced) swap rate can be expressed by

$$\mathrm{d}\tilde{S}_{i,n}(t) = \tilde{S}_{i,n}(t)\sigma^{S}_{i,n}\mathrm{d}W(t) \tag{5.9}$$

and thus follows

$$\begin{aligned}\sigma^S_{i,n} &\approx \sum_{k=i}^{n} \frac{\tilde{F}(t,T_k,T_{k+1})}{\tilde{S}_{i,n}(t)}\omega_k(t_0)\tilde{\sigma}_k \\ &\approx \sum_{k=i}^{n} \frac{\tilde{F}(t_0,T_k,T_{k+1})}{\tilde{S}_{i,n}(t_0,t)}\omega_k(t_0)\tilde{\sigma}_k \end{aligned} \tag{5.10}$$

Now, the EPE is given by

$$\begin{aligned} EPE(t_0,t,T_n) &= V^{\text{swpt}}(t_0,t,T_n,T_n) \\ &= V_c^{\text{Black}}(0,t,\tilde{S}_{i,n}(t_0,t),K,\sigma^S_{i,n}) \sum_{k=q(t)}^{N} \tau_k P(t,T_k) \end{aligned} \tag{5.11}$$

For the approximation of the Hull-White EPE, Jamshidian's composition is used [24], which uses the characteristics of a single-curve environment. The Jamshidian's decomposition is given in equation (5.12) and explained in more detail in Appendix C.2.

$$\begin{aligned} V_{\text{swpt}}(t_0,T_i,T_n,T_n) &= \sum_{k=i}^{n} c_i V_p^{\text{zcb}}(t_0,T_i,T_{k+1},X_{i,k}) \\ c_i &= K\tau_i \\ c_n &= 1+K\tau_i \\ X_{i,k} &= \exp\left(A(T_i,T_{k+1}) - B(T_i,T_{k+1})r^*\right) \end{aligned} \tag{5.12}$$

and where r^* can be found by

$$\sum_{k=i}^{n} c_i \exp\left(A(T_i,T_{k+1}) - B(T_i,T_{k+1})r^*\right) = 1 \tag{5.13}$$

To find the zero-coupon bond put price, equation (4.11) is used. The bond volatility, $\text{Var}[P(T_i,T_{i+1})|\mathcal{F}_t]$, is expressed in terms of Hull-White volatilities and given in equation (3.26). Note that the EPE of a swap is equal to the swaption price.

The EPEs are shown in Figure 5.12, with different maturities and different accrual periods. Since the Hull-White EPE estimation uses the properties of a single-curve environment, Figure 5.12 only shows single-curve EPEs. Moreover, the approximation of the Hull-White EPE is only calculated for tenor points. Therefore, it should correspond with the lower points of the simulated Hull-White EPEs.

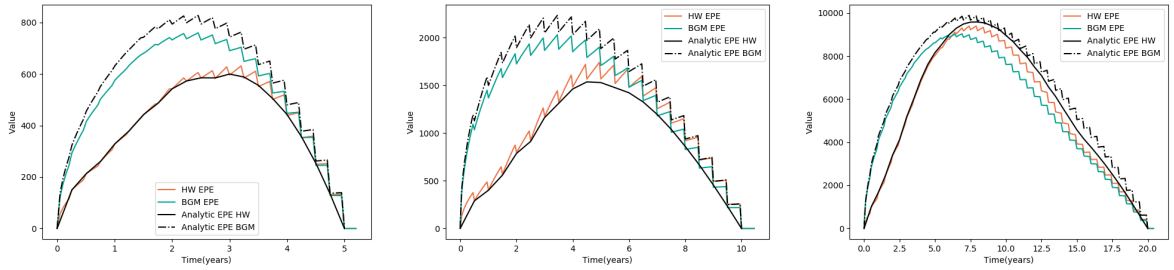

(a) (b) (c)

Figure 5.12: Plots of the analytic swap EPE and the simulated swap EPE of the Hull-White model and BGM model with 100000 paths. (a) a 5-years payer swap with quarterly payments in single curve framework. (b) a 10-years receiver swap with semi-annually payments, in a single curve framework. (c) a 20-years payer swap with semi-annually payments, in a single curve framework.

The EPE calculations are an approximation and are thus not exact. Therefore, the slight difference between the simulated EPE and the calculated EPE that appears is, however, negligible for practical purposes.

6

Comparison

In this chapter, the Hull-White model and BGM model are compared. First, a convergence analysis, computational complexity and computation time are given of both models. Then the swap EPE of both models for different scenarios is presented. Finally, a conclusion is given.

6.1. Computation

6.1.1. Convergence

In this section, we check the convergence of both models. Therefore, we measure the mean-squared error, mean absolute error, maximum absolute error and computation time for a different number of paths of the simulated caplet volatilities. Figure 6.1 (a) and (b) show the mean-squared error and the absolute error of the Hull-White and BGM model for a varying number of paths and a fixed number of time steps and number of forwards. Figure 6.1 (c) shows the computation times per number of paths. Since the error can fluctuate a lot for a small number of paths, the simulation is run 100 times, and for each path, the mean is taken of the mean-squared error and the computation time.

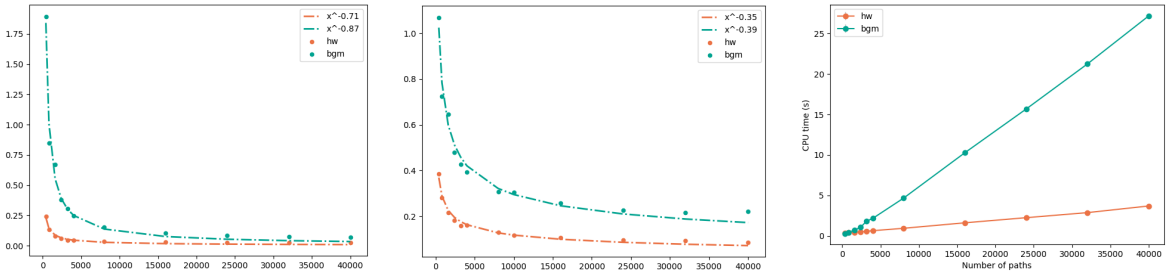

(a) Mean-squared error (b) Absolute error (c) Computation time

Figure 6.1: Plots of the mean-squared error of the simulated caplet volatility and computation time per number of paths for both the Hull-White model and BGM model. The volatilities are in %. For 230 time steps and 42 forwards. For each path the mean is taken over 100 simulations. In (a) and (b) is for both models a power function is fitted through the data points.

Note that only the computation time of the Monte Carlo simulation and the calculation of the caplet volatilities is taken into account (not the calibration). In Figure 6.1, it is shown that the Hull-White model has both a smaller error and a shorter computation time per number of paths than the BGM model. The computation of both the Hull-White model and BGM model increase linearly. Furthermore, a characteristic of the Monte Carlo simulation is that it converges with a factor $\sqrt{\#\text{ paths}}$ [26]. Figure 6.1 (a) and (b) the MSE and absolute error with a fitted line through the points, which shows that they converges approximately by a factor $\sqrt{\#\text{ paths}}$. The power of the fitted line can change a little if another set of data points is chosen. For the Hull-White, the convergence slows down around the data point of 16000 paths and, for the BGM model, around the data points of 24000 or 32000 paths. Therefore, we will compare the swap MTM and EPE of both models for 25000 paths.

6.1.2. Computational complexity

For the computational complexity section, we explain how the computations are structured and give the calibration and simulation computation time. In each comparison of the computation time, only one input is changed. In such a way, the impact of each component is taken into account.

Calibration Only the Hull-White model has to calibrate its model volatilities. In this calibration, the Hull-White model volatility is found from the market caplet volatility for each accrual period. Therefore, a for loop depends on the number of caplet volatilities and thus a number of forwards. In this for loop, 4 transitions are made; from the caplet volatility to the caplet price, to the zero-coupon bond price to the zero-coupon bond volatility to the Hull-White model volatility, as shown in Figure 4.2. Where in each loop on integer level multiplications and additions and subtractions are done, see the formula mentioned in Figure 4.2. Therefore, the more expiry dates per swap, the longer the calibration will be. Both for local and global calibration, the computation time for a different number of expiry dates is given in Figure 6.2.

Figure 6.2 shows that the local calibration computation time grows linearly, and the global optimisation increase linearly until 40 expiry dates, after which it increase considerably faster. The difference between local and global optimisation becomes more evident the more expiry dates are used. For the local optimisation for each extra expiry date, an extra time the for loop has to run. Furthermore, for the global optimisation for each additional forward rate, an extra dimension is added to the optimisation. Note that for global optimisation, local optimisation is used as input.

Simulation In the simulation, the number of paths, the number of time steps and the number of forwards play a role. For the Hull-White short-rate simulation, a for loop is taken over the number of time steps wherein each loop the simulated short-rate is calculated for each path, by vector and integer multiplication, addition and subtraction. For the BGM forward rate simulation, a double for loop is used over the time steps and over the forwards, as each forward has its own dynamics. For each time step, all the forward rates are calculated for each path by vector and integer multiplication, addition and subtraction.

Figure 6.2(b) shows the CPU time for a different number of time steps for both the simulation of the Hull-White short-rate and the BGM forward rates. The paths and number of forwards are set to 10000 paths and 42 forwards and 10 steps per accrual period. In other words, the maximum number of time steps is 420 time steps. Henceforth, for 40 time steps, all the 42 forward rates are considered, and the simulation stops after 40 time steps.

Furthermore, the effect of the different number of forwards on the computation time of the BGM simulated forwards is shown in Figure 6.2(c). In these simulations, 10000 paths and 400 time steps. Therefore, the fewer forwards are simulated, the more time steps per accrual period are used.

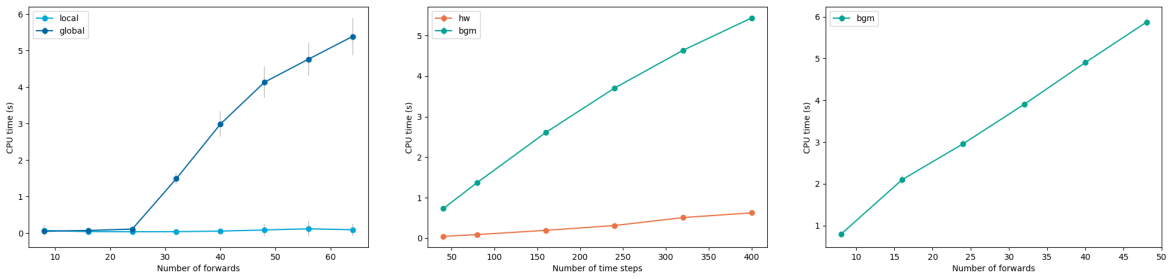

(a) CPU calibration HW (b) CPU simulation HW and BGM (c) CPU simulation BGM

Figure 6.2: Plots of the CPU time of (a) the calibration of the Hull-White model for different number of expiry dates for local and global calibration, where the grey line represents the standard deviation. (b) simulation of the Hull-White short-rates and BGM forward rates for different number of time steps and (c) simulation of BGM forwards for different number of forwards. The CPU times are an average of 100 runs.

Figure 6.2(b) shows that both the computation time of the Hull-White model and the BGM model increase linearly with the number of steps. Moreover, the Hull-White simulation has a lower computation time than the BGM model for the same number of time steps and forwards. Figure 6.2(c) shows that the computation time increases linearly when more forwards are simulated. Note that only one factor changes in all the computation time analyses, and the other factors are constant.

Concluding in that for the same number of forward rates, paths and time steps, the Hull-White model has a lower computation time for the simulation than the BGM model. Besides, the local and global calibration are compared, where from 40 expiry dates, the global calibration increases considerably compared with the local calibration. Note that the given computation times are implementation and computer-dependent and could be improved or optimised. However, it does provide a good reflection of how the computation time increases for larger inputs.

6.2. Comparison

This section will give a comparison of the EPE of different swaps of both models. We will compare different swaps that are ATM, ITM and OTM, receiver and payer swaps and swaps with different tenor-structures and maturities.

First, we consider what happens when a swap is far ITM. Figure 6.3 shows three swaps all with a 1 month accrual period, 2 years maturity and receiving fixed with 100000 paths and 10 steps per accrual period. All three have a different strike with (a) a par strike of -0.00544, (b) a strike of -0.00644 and (c) a strike of -0.01544.

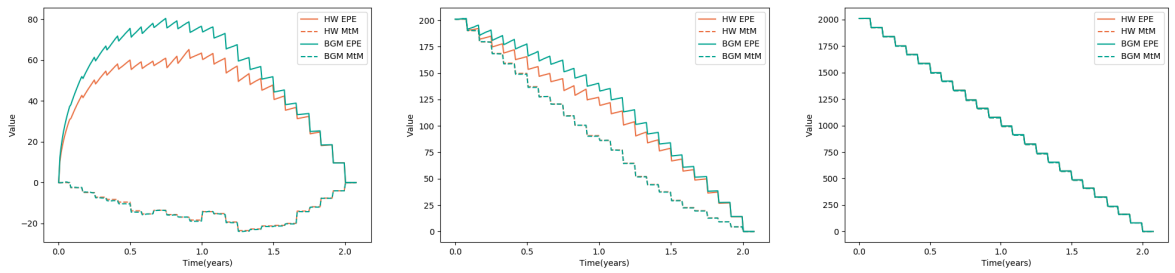

(a) (b) (c)

Figure 6.3: Plots of 2 year receiver swap with monthly payments with a notional of 100000 and in Figure (a) a par strike of -0.00544, (b) a strike of -0.00644 and (c) a strike of -0.01544.

Figure 6.3 shows that the further the swap is into the money, the closer the EPE is to the MTM. In Figure 6.3 (c), the EPE is equal to the MTM (for both models). Remark that according to equation (2.45), this could be explained by the fact that the maximum of each swap value and zero is equal to the swap value (no paths below zero). Since both models are calibrated to the market curves, the simulated MTM of the swap should be equal to the analytically calculated MTM, see Section 5.2.

Next, consider the EPE of a payer and receiver swap with a 6-months accrual period and a 20-years maturity, in Figure 6.4.

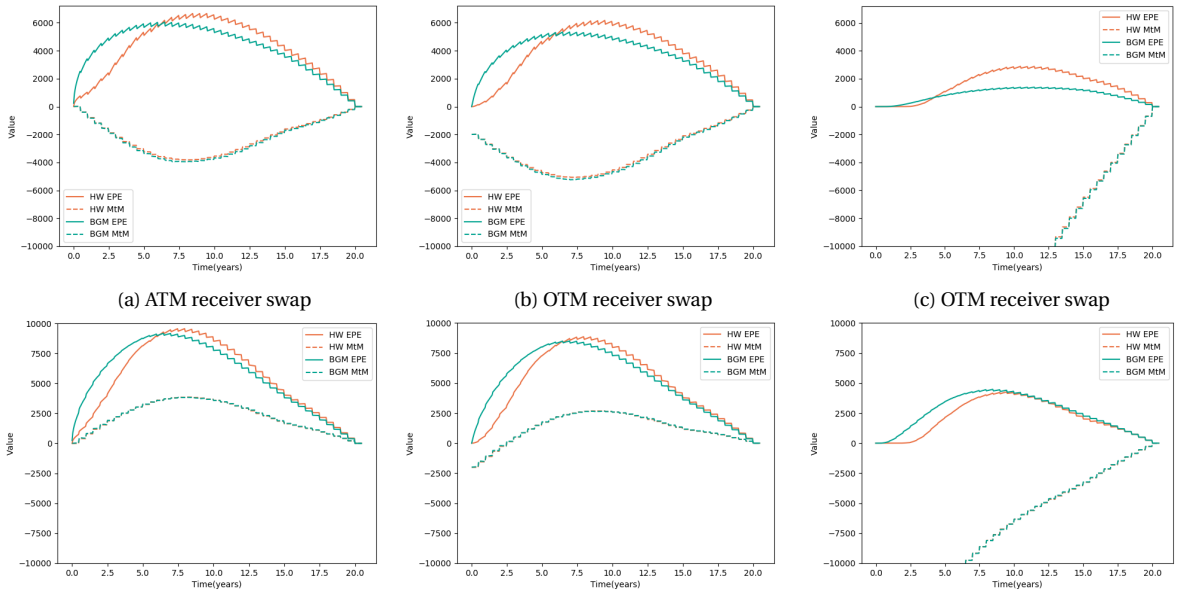

(a) ATM receiver swap (b) OTM receiver swap (c) OTM receiver swap

(d) ATM payer swap (e) OTM payer swap (f) OTM payer swap

Figure 6.4: Plots of of the MTM and EPE of the Hull-White and BGM model of 20-years receiver/payer swap with semi-annual payments with a notional of 100000 and in Figure (a) a par strike of 0.00272, (b) a strike of 0.00172 and (c) a strike of -0.00728. (d) a par strike of 0.00272, (e) a strike of 0.00372 and (f) a strike of 0.01272. The simulation have 100000 paths and 10 steps per accrual period.

Figure 6.4 shows the EPE and MTM of the Hull-White and BGM model of the swap for different ATM and OTM strikes. Where the MTM is plotted to show how far the swap is out of the money. In Figure 6.4 (c) and Figure 6.4 (f), the MTM is partly outside the shown plot. However, since we want to compare the EPE the exact value of the MTM is not of importance.

Moreover, Figure 6.5 shows the swap rate distribution of this 20-years swap with semi-annually payments. The distribution of both the Hull-White and BGM model is shown for 2-years, 5-years and 15-years.

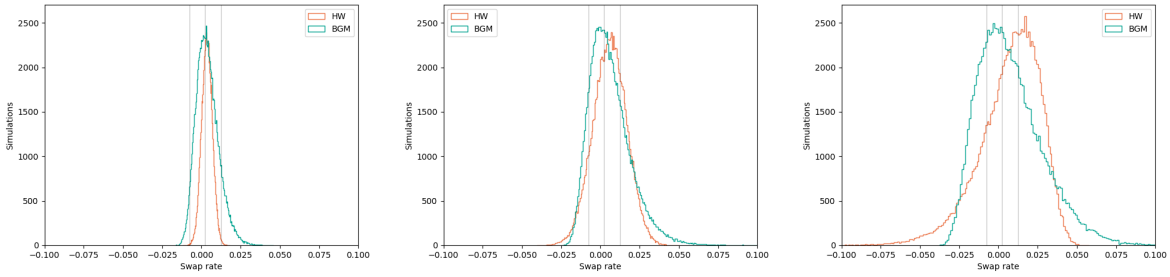

(a) 2 years (b) 5 years (c) 15 years

Figure 6.5: Plots of the swap rate distribution of a 2 year swap with semi-annually payments and a notional of 100000 at time (a) 5 years, (b) 10 years, (c) 15 years of the Hull-White and BGM model. The vertical lines are the par strike of 0.0027 and the OTM strikes -0.00728, 0.01272

Figure 6.5 shows that the distributions for the BGM model are skewed to the right and start around -0.03 (the value of the displacement), similarly to a displaced log-normal distribution. The Hull-White distributions are symmetric in the first number of years, likewise to the normal distribution, and start to become more left skewed, see Figure 6.5 (c). Moreover, the further the simulation, the wider the distribution becomes, as the paths spread out more. Recall the formula for the swap rate in equation (2.28). From this formula, one can find that the left tail of the swap rate distribution is essential for the receiver swap EPE and the right tail for the payer swap EPE. Therefore, for far OTM swaps, the tails are evident in the EPE. For a far OTM receiver swap, the left tail is of importance. The left tail of the Hull-White distribution is fatter than that of the BGM model, see Figure 6.5 (b)-(c). Therefore, the EPE of the Hull-White at time 10-years and 15-years is higher than that of the BGM model, see Figure 6.4 (c). For a far OTM payer swap, the right tail is of importance. In Figure 6.5 (a), the BGM model has a larger tail than the Hull-White model. Figure 6.4 (f) shows this effect, where at time 5-years, the EPE of the Hull-White model is lower than that of the BGM model.

Figure 6.6 shows the MTM and EPE of the Hull-White and BGM model of a 3-years swap with quarterly payments.

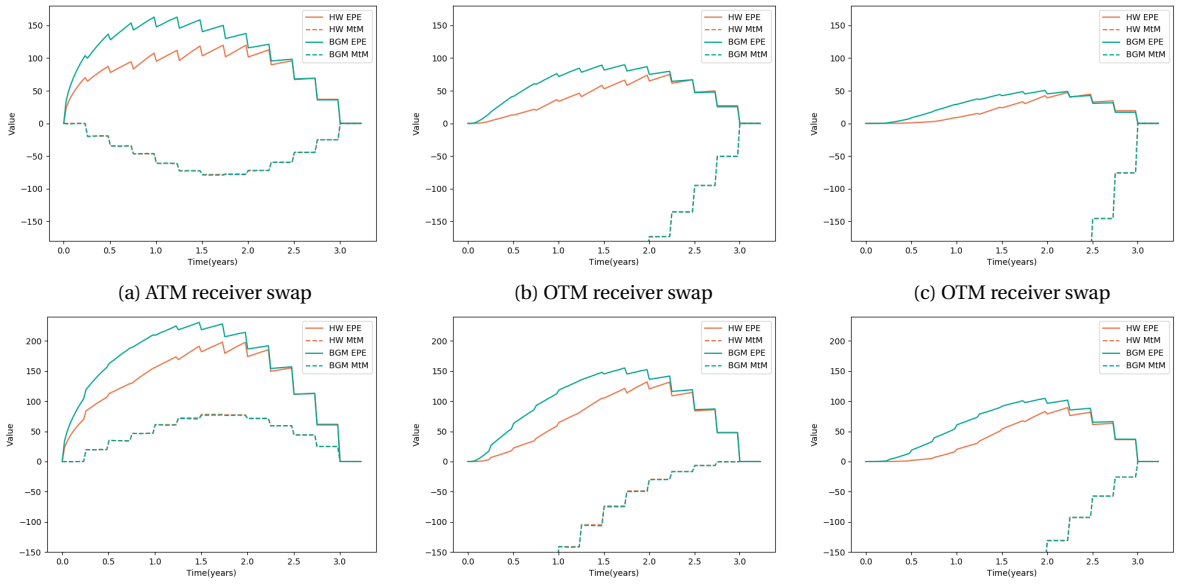

(a) ATM receiver swap (b) OTM receiver swap (c) OTM receiver swap

(d) ATM payer swap (e) OTM payer swap (f) OTM payer swap

Figure 6.6: Plots of of the MTM and EPE of the Hull-White and BGM model of a 3 year receiver/payer swap with quarterly payments and a notional of 100000 and in Figure (a) a par strike of -0.0048457, (b) a strike of -0.0058457 and (c) a strike of -0.0068457.(d) a par strike of -0.0048457, (e) a strike of -0.0038457 and (f) a strike of -0.0028457.

The swap rate distributions of the swaps of Figure 6.6 is given in Figure 6.7 for 0.5-year, 1-year and 2-years.

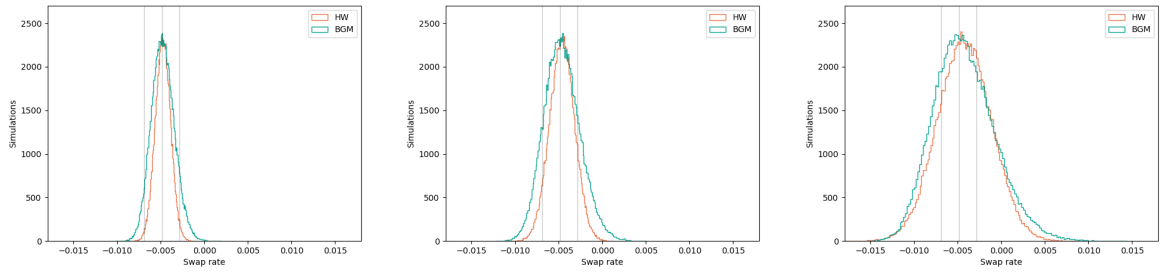

(a) 0.5 years (b) 1 years (c) 2 years

Figure 6.7: Plots of the swap rate distribution of a 3 year swap with quarterly payments and a notional of 100000 at time (a) 0.5 years, (b) 1 years, (c) 2 years of the Hull-White and BGM model. The vertical lines are the par strike of -0.0048457 and the OTM strikes -0.0028457, -0.0068457

The swap-rate distribution in Figure 6.7 shows that the BGM model has fatter-tails than the Hull-White model on both sides. In Figure 6.6, this results in a lower EPE for the Hull-White model respective to the BGM model.

Furthermore, consider a two year swap with yearly payments. The first payment is fixed at time zero and the second payment is fixed at 1 year, shown in Figure 6.8.

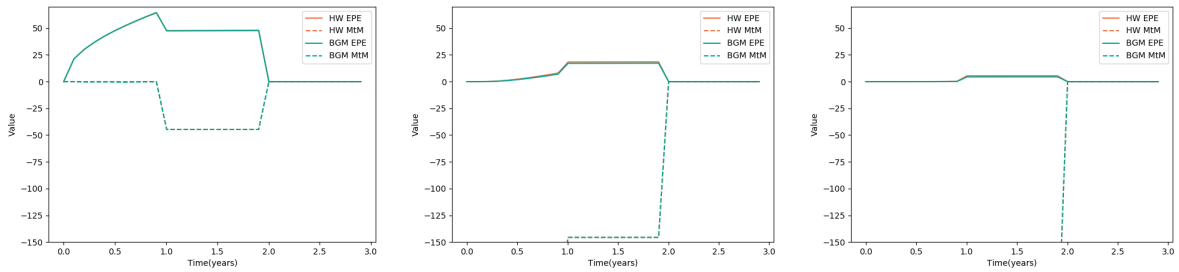

(a) atm (b) otm (c) far otm

Figure 6.8: Plots of the swap rate distribution of a 3 year swap with quarterly payments and a notional of 100000 at time (a) 0.5 years, (b) 1 years, (c) 2 years of the Hull-White and BGM model. The vertical lines are the par strike of -0.0048457 and the OTM strikes -0.0028457, -0.0068457

The swap rate distributions of this swap for different times are shown in Figure 6.9.

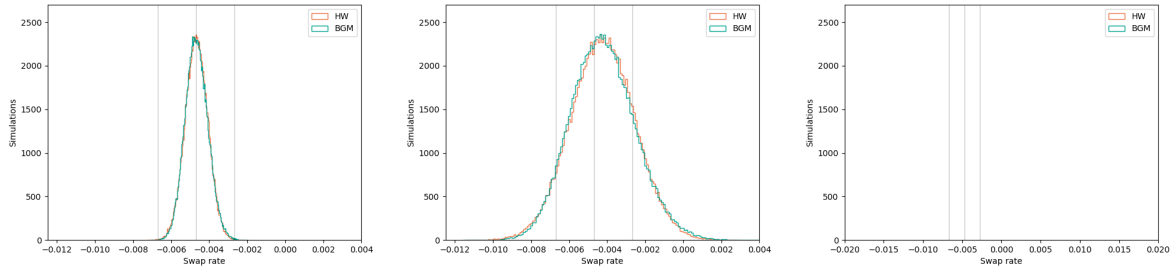

(a) 0.5 years (b) 1 years (c) 2 years

Figure 6.9: Plots of the swap rate distribution of a 2 years swap with annual payments (a) atm, (b) 1 years, (c) 2 years of the Hull-White and BGM model. The vertical lines are the par strike of -0.0048457 and the OTM strikes -0.0028457, -0.0068457

Figure 6.8 and Figure 6.9 show that the EPE and the swap rate distributions are equal for the Hull-White and BGM model. Remark that both models are calibrated to caplets and that the EPE of a swap with a single payment is equal to the caplet value. Indeed, as for a single payment, the swap rate is equal to the forward; see equation (2.28). Henceforth, the swaption value is equal to the caplet value, equation (2.33) and (2.39). Moreover, this is again confirmed if we inspect the analytic approximation of the EPE for both models. The analytic approximation of the swap EPE in the Hull-White model is given

in equation (5.12). For a single payment, this becomes

$$V_{\text{swpt}}(t_0, T_i, T_{i+1}, T_{i+1}) = (1 + K\tau_i)V_p^{\text{zcb}}(t_0, T_i, T_{i+1}, X_{i,i+1}) \tag{6.1}$$

$$X_{i,i+1} = \frac{1}{1 + K\tau_i} \tag{6.2}$$

which is equal to the caplet price, equation (4.10). Moreover, the analytic approximation of the swap EPE in the BGM model is given in equation (5.5). For a single payment the swap rate volatility is equal to the forward rate volatility, and thus the caplet volatility. Therefore, by equation (5.11) the swaption is equal to the caplet price.

In Figure 6.10, a swap portefolio with 10 swaps is considered, where the swaps have different maturities and payment structures.

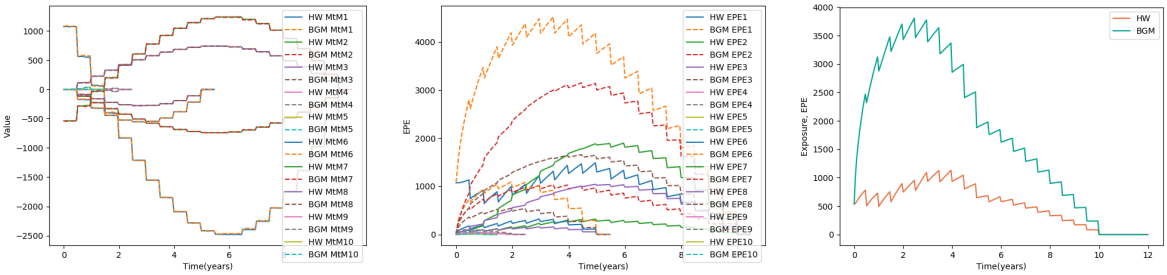

(a) MtM (b) EPE (c) Netted EPE

Figure 6.10: Plots of swap portfolio with 10 different swaps. Where swap 1-6 are receiver swaps and swap 7-10 are payer swaps. Swap 4,5,9 are quarterly paying swaps and the rest are semi-annually paying swaps. Swap 1,5,6 have a notional of 200000, swap 3,7,9 of 100000 and swap 2,4,8,10 of 50000. (a) the MtM (solid) of the individual swaps for the Hull-White and BGM (dashed) model. (b) the EPE (solid) of the individual swaps for the Hull-White and BGM (dashed) model. (c) the netted EPE of the swap portfolio of both models.

Figure 6.10 (a) shows that indeed the MTM of the swaps are the same for both models. Figure 6.10 (b) and (c) show the EPE of the individual swaps and the netted EPE of the whole portfolio. The figure shows that the EPE of a portfolio can be significantly different for both models.

Concluding with that Hull-White model and the BGM model give a different EPE in most situations. Only for a single payment swap and for a far ITM swaps, both models give the same EPE. Figure 6.5, Figure 6.7 and Figure 6.9 show the difference for both models in the swap rate distributions, where the Hull-White model is more centred than the BGM model. Moreover, the BGM model has larger right skewness, similar to that of a log-normal distribution. The more extreme cases occur in the swap rate distribution, the higher a far OTM swap EPE is. Therefore, the tails of swap rate distribution should correspond with market expectations. A tail that is not fat enough might underprice far OTM swap EPEs and the other way around. The key takeaway is that there is a model risk when choosing between the Hull-White model and the BGM model, as they give different results for the EPE; definition 2.3.5. This model risk could be incorporate in for example the model risk AVA, defined in definition 2.3.6.

7

Conclusion

Since the appearance of negative interest rates, the use of log-normal models has come under re-considerations. Henceforth, the disadvantage of normally distributed interest rate models becomes their advantage; the possibility of negative rates. Furthermore, since the financial crisis in 2008, increased importance around credit risk has risen, which includes the credit validation adjustment (CVA) and expected positive exposure (EPE).

Therefore, the aim of this thesis was to give a comparison of the Hull-White and BGM model on the EPE of a swap portfolio. Both models were chosen to be multi-curve, single-currency and calibrated to caplets. The mean-reversion parameter was left out of the Hull-White model to compare both models on a similar level. For both models, a Monte Carlo simulation has been carried out, from where the EPE of the swaps is calculated. The models will be compared on the convergence, computation time and EPE.

The Hull-White model is a model that simulates the short-rate with a normal distribution. Since it has a normal distribution, it can incorporate negative rates. Furthermore, one of the advantages of the Hull-White model is that it has a closed-form solution for the zero-coupon bond, given in equation (3.14). For the calibration of the Hull-White model to caplet volatilities, multiple steps are needed. First, with the market caplet volatility, the caplet price is calculated. After that, the zero-coupon bond put prices are found. Next, the zero-coupon bond put volatility is determined. Last, the implied market zero-coupon bond variance is set equal to that of the analytic Hull-White zero-coupon variance, with which the Hull-White model volatilities are found; see Figure 4.2. For the calibration, local optimisation is introduced with bootstrapping. In the local optimisation in some situations, the optimal Hull-White variance would be negative variance, which is not possible. Therefore, two methods are proposed to solve this problem; one is a global optimisation on the Hull-White volatilities, which minimises the mean-squared error. Another is by smoothing the discounting/forecasting curve, which is used as input for the calibration. Moreover, Monte Carlo simulation is used to simulate the Hull-White short-rate. We suggest using an analytical integration instead of Euler's discretisation method, such that the simulation is not dependent on the step size of the discretisation.

Whereas the BGM model is a model which simulates the forward rates, where each forward rate has its own dynamics, and all follow a log-normal distribution. Since a log-normal distribution does not have negative random variables and thus negative forward rates can not be incorporated, a displacement is used. For the BGM model the market caplet volatilities can directly be used model volatilities, where each forward is driven by a corresponding constant caplet volatility. In the Monte Carlo simulation of the BGM forward, Eulers discretisation is used, since it is not possible to find an analytic solution for the integration. The discount factors of the BGM simulation are found by multiplication using the forward rates and an interpolation technique; described in equation (3.44).

Furthermore, we introduce a way to incorporate multiple discounting/forecasting curves by using the spreads between the curves. For the BGM model, the same technique can be used when there are in a swap portfolio swaps with forwards with different payments structures. For example, if a 6-months forward is simulated, first, the discount factors are found and then these discount factors are multiplied with the spread to find the 3-months forecast factors. Last, the 3-months forward can be found with these forecast factors and the forward rate definition.

To validate that the models are correctly implemented the models are tested to price back the caplet volatilities, the discounting curve, the MTM of single swap and the EPE of a single swap. For the EPE an approximation is made for both models. For the BGM model the approximation is made using the fact that the swap rate can be given by a weighted sum of forward rates, which is used to find the swap rate volatility and therefore the swaption price (or EPE); equation (5.11). For the Hull-White model the approximation of the EPE is made by Jamshidian's decomposition, which states that the

swaption price can be given by a weighted sum of zero-coupon bond puts prices. Where the strikes of the zero-coupon bond put price can be determined using the Hull-White closed form solution of the zero-coupon bond; equation (5.12).

To compare both models, we inspect the convergence, the computation time and the EPE. We found that the Hull-White model both has a faster convergence as a shorter computation time for different inputs than the BGM model. Note that this is implementation dependent. Moreover, the EPE of both models were compared, where for a single payment swap and for far ITM swap EPEs, both models give the same EPE. The EPE of a single payment swap is equal to the swaption value of the single payment swap, which is the caplet value. Since both models are calibrated to the same caplets the EPE is the same. The EPE of far ITM swaps is the same since these become equal to the MTM, which are the same as both models are calibrated tot the market curves. For the other compared swaps, the EPEs of both models differ and can be explained by the distribution of the swap rate. The swap rate distribution of the BGM model has fatter tails and more right-skewed than the Hull-White model. The left tail of the swap rate distribution tells us something about the receiver swaps and the right tail of the distribution of the payer swaps. Especially for far OTM swaps, the tails are of great importance. If a tail of the swap rate distribution is fatter than it should be according to the market, the EPE is overpriced, and if it is less fat, it might be underpriced. Since the interest rate is not limited by zero or any other number, the model should incorporate the possibility of negative rates. In the BGM model, this could be done by a displacement. However, this displacement still limits the left tail of the distribution of the forward rates and thus the swap rates distribution.

We limited the research question to a single currency model and chose to calibrate to caplets. Therefore, we would recommend for further research to look into a multi-currency model and the possibility of calibrating to swaptions. In particular, the calibration to swaptions might be more appealing for a single swap or a small swap portfolio, as the swaption value gives the EPE of the underlying swap. Furthermore, one could research a more advanced multi-curve framework. An option could be to have a framework where each discounting or forecasting curve is simulated with its own dynamics and a mutual correlation. A disadvantage of this framework would be that it has a higher computation time.

In conclusion, the key takeaway found in this thesis is that there is a difference between the EPE of the Hull-White model and the BGM model. This difference causes that there is model risk in choosing between both models. This model risk could be incorporated in, for example, the model risk AVA, defined in definition 2.3.6. If we should recommend which model is best to use, our personal preference will be the Hull-White model because of the lower bound of the BGM model. However, it is difficult to quantify what the "best" EPE is, and the most important message is that one should not ignore the risks of a specific model choice.

Bibliography

[1] Ametrano, F. M. and Bianchetti, M. (2013). Everything you always wanted to know about multiple interest rate curve bootstrapping but were afraid to ask. *SSRN Electronic Journal*.

[2] Bera, C. M. J. . A. K. (1980). Efficient tests for normality, homoscedasticity and serial independence of regression residuals. *Economics Letters*, 6(3):255–259.

[3] Bianchetti, M. (2008). Two curves, one price: Pricing & hedging interest rate derivatives decoupling forwarding and discounting yield curves. *SSRN Electronic Journal*.

[4] Black, F. and Karasinski, P. (1991). Bond and option pricing when short rates are lognormal. *Financial Analysts Journal*, 47:52–59.

[5] Brace, A. (2008). *Engineering BGM*. Chapman and Hall/CRC.

[6] Brace, A., Gątarek, D., and Musiela, M. (1997). The market model of interest rate dynamics. *Mathematical Finance*, 7(2):127–147.

[7] Brigo, D. and Mercurio, F. (2006). *Interest Rate Models - Theory and Practice: With Smile, Inflation and Credit*. Springer Finance.

[8] Bühler, W., Uhrig-Homburg, M., Walter, U., and Weber, T. (1999). An empirical comparison of forward-rate and spot-rate models for valuing interest-rate options. *Journal of Finance*, 54:269–305.

[9] Cirillo, P. (2020). Financial mathematics. *TU Delft*.

[10] Cox, J., Ingersoll, J., and Ross, S. (1985). A theory of the term structure of interest rates. *Econometrica*, 53 (2):385–407.

[11] Danielsson, J., James, K. R., Valenzuela, M., and Zer, I. (2016). Model risk of risk models. *Journal of Financial Stability*, 23:79–91.

[12] Dekking, F., Kraaikamp, C., Lopuhaä, H. P., and Meester, L. E. (2005). *A Modern Introduction to Probability and Statistics: Understanding Why and How*. Springer.

[13] European Banking Authority (2015). Eba final draft regulatory technical standards. *European Banking Authority*.

[14] FINCAD (2011). Basics of credit value adjusments and implications for the assessment of hedge effectiveness.

[15] Gurrieri, S., Nakabayashi, M., and Wong, T. (2009). Calibration methods of Hull-White model. *SSRN*.

[16] Hagan, P. S. and West, G. (2006). Interpolation methods for curve construction. *Applied Mathematical Finance*, 13(2):89–129.

[17] Heath, D., Jarrow, R., and Morton, A. (1992). Bond pricing and the term structure of interest rates: A new methodology for contingent claims valuation. *Econometrica*, 60(1):77–105.

[18] Ho, T. and Lee, S.-B. (1986). Term structure movements and pricing interest rate contingent claims. *Journal of Finance*, 41(5):1011–1029.

[19] Hull, J. and White, A. (1990). Pricing interest-rate-derivative securities. *The review of Financial Studies*, 3(4):573–592.

[20] Hull, J. and White, A. (1994). Numerical procedures for implementing term structure models I: Single-factor models. *Journal of Derivatives, Fall*, 2(1):7–16.

[21] Hull, J. and White, A. (2000). Forward rate volatilities, swap rate volatilities, and implementation of the LIBOR market model. *The Journal of Fixed Income*, 10(2):46–62.

[22] Ilgmann, C. and Menner, M. (2011). Negative nominal interest rates: History and current proposals. *International Economics and Economic Policy*, 8:383–405.

[23] ISDA (2020). Key trends in the size and composition of OTC derivatives markets in the second half of 2019. *ISDA*.

[24] Jamshidian, F. (1989). An exact bond option pricing formula. *The Journal of Finance*, 44:205–209.

[25] Mercurio, F. (2018). A simple multi-curve model for pricing SOFR futures and other derivatives. *SSRN Electronic Journal*.

[26] Oosterlee, C. W. and Grzelak, L. A. (2020). *Mathematical Modeling and Computation in Finance*. World Scientific Publishing Europe Ltd.

[27] Pelsser, A. (1997). A tractable yield-curve model that guarantees positive interest rates. *Review of Derivatives Research*, 1:269–284.

[28] Pelsser, A. and Moraleda, J. (1997). Forward versus spot interest-rate models of the term structure: An empirical comparison. *The Journal of Derivatives*, Spring.

[29] Riga, C. (2010). The LIBOR market model: from theory to calibration. Master's thesis, Universita di ' Bologna, FACOLTA DI SCIENZE MATEMATICHE.

[30] Ritchken, P. and Sankarasubramanian, L. (2004). A multifactor model of the quality option in treasury futures contracts. *Journal of Financial Research*, 18:261–79.

[31] Savitzky, A. and Golay, M. (1964). Smoothing and differentiation of data by simplified least squares procedures. *Analytical Chemistry*, 36(8):1627–1964.

[32] ter Bogt, B. (2018). Arbitrage-free interpolation in the LIBOR market model. Master's thesis, Department of Econometrics, University of Amsterdam.

[33] Vasicek, O. (1977). An equilibrium characterization of the term structure. *Journal of Financial Economics*, 5:177–188.

[34] Zhu, J. (2012). Multiple-curve valuation with one-factor Hull-White model. *SSRN Electronic Journal*.

A

Appendix A: Hull-White parameter theta

For theta to fit the initial term structure, we use the closed form of the zero-coupon bond under the Hull-White model and the fact that the zero-coupon bond of the market is equal to the zero coupon bond of the model:

$$e^{-\int_{t_0}^{t} f^r(t_0,s)\mathrm{d}s} = P^M(t_0,t) = P^{HW}(t_0,t) = e^{-\int_0^t r^{HW}(s)\mathrm{d}s} \tag{A.1}$$

with $f^r(t_0,t)$ the instantaneous forward rate and $r(t)$ the short-rate. It follows that

$$\theta(t) = \frac{\partial f^r(t_0,t)}{\partial t} + \alpha f^r(t_0,t) + \frac{1}{2}\left(\frac{\partial^2\left(\mathrm{Var}\left[\int_{t_0}^t r(s)\mathrm{d}s\middle|\mathscr{F}_{t_0}\right]\right)}{\partial^2 t} + \alpha\frac{\partial\left(\mathrm{Var}\left[\int_{t_0}^t r(s)\mathrm{d}s\middle|\mathscr{F}_{t_0}\right]\right)}{\partial t}\right) \tag{A.2}$$

A.1. Theta parameter with mean-reversion

The integrated short-rate variance is given by

$$\mathrm{Var}\left[\int_{t_0}^t r(s)\mathrm{d}s\middle|\mathscr{F}_{t_0}\right] = \int_{t_0}^t \frac{\sigma_{hw}^2(s)}{\alpha^2}(1-e^{-\alpha(t-s)})^2\mathrm{d}s \tag{A.3}$$

Using Leibniz integration rule, $\frac{\partial}{\partial t}\int_a^t f(s,t)\mathrm{d}s = f(t,t) + \int_a^t \frac{\partial}{\partial t}f(s,t)\mathrm{d}s$, the derivative becomes:

$$\begin{aligned}\frac{\partial\left(\mathrm{Var}\left[\int_{t_0}^t r(s)\mathrm{d}s\middle|\mathscr{F}_{t_0}\right]\right)}{\partial t} &= \frac{\partial}{\partial t}\int_{t_0}^t \frac{\sigma_{hw}^2(s)}{\alpha^2}(1-e^{-\alpha(t-s)})^2\mathrm{d}s \\ &= \frac{\sigma_{hw}^2(t)}{\alpha^2}(1-e^{-\alpha(t-t)})^2 + \int_{t_0}^t \frac{\partial}{\partial t}\frac{\sigma_{hw}^2(s)}{\alpha^2}(1-e^{-\alpha(t-s)})^2\mathrm{d}s \\ &= \int_{t_0}^t \frac{\sigma_{hw}^2(s)}{\alpha^2}(2\alpha e^{-\alpha(t-s)} - 2\alpha e^{-2\alpha(t-s)})\mathrm{d}s\end{aligned} \tag{A.4}$$

Again, differentiating:

$$\begin{aligned}\frac{\partial^2\left(\mathrm{Var}\left[\int_{t_0}^t r(s)\mathrm{d}s\middle|\mathscr{F}_{t_0}\right]\right)}{\partial^2 t} &= \frac{\partial}{\partial t}\int_{t_0}^t \frac{\sigma_{hw}^2(s)}{\alpha^2}(2\alpha e^{-\alpha(t-s)} - 2\alpha e^{-2\alpha(t-s)})\mathrm{d}s \\ &= \frac{\sigma_{hw}^2(t)}{\alpha^2}(2\alpha e^{-\alpha(t-t)} - 2\alpha e^{-2\alpha(t-t)}) + \int_{t_0}^t \frac{\partial}{\partial t}\frac{\sigma_{hw}^2(s)}{\alpha^2}(2\alpha e^{-\alpha(t-s)} - 2\alpha e^{-2\alpha(t-s)})\mathrm{d}s \\ &= \int_{t_0}^t \frac{\sigma_{hw}^2(s)}{\alpha^2}(-2\alpha^2 e^{-\alpha(t-s)} + 4\alpha^2 e^{-2\alpha(t-s)})\mathrm{d}s\end{aligned} \tag{A.5}$$

Therefore, it follows with substitution in equation (A.2) that theta is given by

$$\theta(t) = \frac{\partial f^r(t_0,t)}{\partial t} + \alpha f^r(t_0,t) + \int_{t_0}^t \sigma_{hw}^2(s)e^{-2\alpha(t-s)}\mathrm{d}s \tag{A.6}$$

A.2. Theta parameter with zero mean-reversion

The integrated short-rate variance is given by

$$\mathrm{Var}\left[\int_{t_0}^{t} r(s)\mathrm{d}s \middle| \mathscr{F}_{t_0}\right] = \int_{t_0}^{t} \sigma_{hw}^2(s)(t-s)^2\mathrm{d}s \tag{A.7}$$

Using Leibniz integration rule, $\frac{\partial}{\partial t}\int_a^t f(s,t)\mathrm{d}s = f(t,t) + \int_a^t \frac{\partial}{\partial t} f(s,t)\mathrm{d}s$, the derivative becomes:

$$\begin{aligned}\frac{\partial\left(\mathrm{Var}\left[\int_{t_0}^{t} r(s)\mathrm{d}s \middle| \mathscr{F}_{t_0}\right]\right)}{\partial t} &= \frac{\partial}{\partial t}\int_{t_0}^{t} \sigma_{hw}^2(s)(t-s)^2\mathrm{d}s \\ &= \int_{t_0}^{t} \sigma_{hw}^2(t)(t-t)^2\mathrm{d}s + \int_{t_0}^{t}\frac{\partial}{\partial t}\int_{t_0}^{t} \sigma_{hw}^2(s)(t-s)^2\mathrm{d}s\mathrm{d}s \\ &= \int_{t_0}^{t}\int_{t_0}^{t} \sigma_{hw}^2(s)(2t-2s)\mathrm{d}s\mathrm{d}s \end{aligned} \tag{A.8}$$

Again, differentiating:

$$\begin{aligned}\frac{\partial^2\left(\mathrm{Var}\left[\int_{t_0}^{t} r(s)\mathrm{d}s \middle| \mathscr{F}_{t_0}\right]\right)}{\partial^2 t} &= \frac{\partial}{\partial t}\int_{t_0}^{t}\int_{t_0}^{t} \sigma_{hw}^2(s)(2t-2s)\mathrm{d}s\mathrm{d}s \\ &= \sigma_{hw}^2(t)(2t-2t) + \int_{t_0}^{t}\frac{\partial}{\partial t}\sigma_{hw}^2(s)(2t-2s)\mathrm{d}s \\ &= 2\int_{t_0}^{t} \sigma_{hw}^2(s)\mathrm{d}s \end{aligned} \tag{A.9}$$

Therefore, it follows that theta is given by

$$\theta(t) = \frac{\partial f^r(0,t)}{\partial t} + \int_{t_0}^{t} \sigma_{hw}^2(s)\mathrm{d}s \tag{A.10}$$

B

Appendix B: Simulation

B.1. Simulation Hull-White model with mean-reversion

B.1.1. Interest-rate simulation

The simulation of the interest-rate, $r(t)$, for the Hull-White model is described in section 4.1.1. In this section is described how $y(t) = r(t)e^{\alpha t}$ can be simulated using the integration of the drift term and the diffusion term and where each step is given by

$$y(t+\Delta) = y(t) + \int_t^{t+\Delta} \theta(s)e^{\alpha s}\mathrm{d}s + \sqrt{\int_t^{t+\Delta} \sigma^2(s)e^{2\alpha s}\mathrm{d}s} \cdot Z \tag{B.1}$$

Now, the drift term, $\int_t^{t+\Delta} \theta(s)e^{\alpha s}\mathrm{d}s$, is a deterministic function and can be calculated analytically. The analytic solution for each time step is given by

$$\begin{aligned}
\int_t^{t+\Delta} \theta(s)e^{\alpha s}\mathrm{d}s &= \int_t^{t+\Delta} e^{\alpha s}\left(\frac{\partial f^r(0,s)}{\partial s} + \alpha f^r(0,s) + \int_{t_0}^{s} \sigma^2(u)e^{-2\alpha(s-u)}\mathrm{d}u\right)\mathrm{d}s \\
&= \left[e^{\alpha s} f^r(0,s)\right]_t^{t+\Delta} + \int_t^{t+\Delta} e^{\alpha s}\left(-\alpha f^r(0,s) + \alpha f^r(0,s) + \int_{t_0}^{s} \sigma^2(u)e^{-2\alpha(s-u)}\mathrm{d}u\right)\mathrm{d}s \\
&= \left[e^{\alpha s} f^r(0,s)\right]_t^{t+\Delta} + \int_t^{t+\Delta} e^{\alpha s}\int_{t_0}^{s} \sigma^2(u)e^{-2\alpha(s-u)}\mathrm{d}u\mathrm{d}s \\
&= \left[e^{\alpha s} f^r(0,s)\right]_t^{t+\Delta} + \int_t^{t+\Delta} e^{-\alpha s}\left(\int_t^{s} \sigma^2(u)e^{2\alpha u}\mathrm{d}u + \int_{t_0}^{t} \sigma^2(u)e^{2\alpha u}\mathrm{d}u\right)\mathrm{d}s
\end{aligned} \tag{B.2}$$

where, in the second line, partial integration is used. Next, we use the fact that $\sigma(s)$ is constant on $[t, t+\Delta)$. However, if only the last integration point is changed, results would not change. Thus, we can assume it constant on the closed interval $[t, t+\Delta]$ and equal to $\sigma(t)$. Therefore, equation (B.2) becomes:

$$\begin{aligned}
\int_t^{t+\Delta} \theta(s)e^{\alpha s}\mathrm{d}s &= \left[e^{\alpha s} f^r(0,s)\right]_t^{t+\Delta} + \int_t^{t+\Delta} e^{-\alpha s}\left(\frac{\sigma^2(t)}{2\alpha}\left(e^{2\alpha s} - e^{2\alpha t}\right) + \sum_{k=0}^{i-1}\frac{\sigma^2(t_k)}{2\alpha}\left(e^{2\alpha t_{k+1}} - e^{2\alpha t_k}\right)\right)\mathrm{d}s \\
&= \left[e^{\alpha s} f^r(0,s)\right]_t^{t+\Delta} + \int_t^{t+\Delta} \frac{\sigma^2(t)}{2\alpha}\left(e^{\alpha s} - e^{-\alpha s + 2\alpha t}\right) + e^{-\alpha s}\sum_{k=0}^{i-1}\frac{\sigma^2(t_k)}{2\alpha}\left(e^{2\alpha t_{k+1}} - e^{2\alpha t_k}\right)\mathrm{d}s \\
&= e^{\alpha(t+\Delta)} f^r(0,t+\Delta) - e^{\alpha t} f^r(0,t) + \frac{\sigma^2(t)}{2\alpha^2}\left(e^{\alpha(t+\Delta)} - 2e^{\alpha t} + e^{-\alpha(t+\Delta)+2\alpha t}\right) \\
&\quad - \left(e^{-\alpha(t+\Delta)} - e^{-\alpha t}\right)\sum_{k=0}^{i-1}\frac{\sigma^2(t_k)}{2\alpha^2}\left(e^{2\alpha t_{k+1}} - e^{2\alpha t_k}\right)
\end{aligned} \tag{B.3}$$

B.1.2. Money-market account simulation

Next, the money-market account, defined in equation (2.21), under the Hull-White model can be found by using equations (3.12),(3.16),(3.15) the closed form of the money market account is given by

$$\begin{aligned} M(t) &= \mathbb{E}\left[\exp\left(\int_{t_0}^{t} r(s)\mathrm{d}s\right)\middle|\mathscr{F}_t\right] \\ &= \exp\left(\frac{r(t_0)}{\alpha}\left(1-e^{-\alpha(t-t_0)}\right)+\int_{t_0}^{t}\frac{\theta(s)}{\alpha}\left(1-e^{-\alpha(t-s)}\right)\mathrm{d}s+\int_{t_0}^{t}\frac{\sigma_{hw}(s)}{\alpha}\left(1-e^{-\alpha(t-s)}\right)\mathrm{d}W(s)\right) \\ &= \exp\left(r(t_0)B(t_0,t)+\int_{t_0}^{t}\theta(s)B(s,t)\mathrm{d}s+\int_{t_0}^{t}\sigma_{hw}(s)B(s,t)\mathrm{d}W(s)\right) \end{aligned} \tag{B.4}$$

Therefore, in a similar way as the interest rate, $r(t)$, the logarithm of the money-market account is simulated simultaneously by

$$\log(M(t+\Delta)) = \log(M(t)) + B(t,t+\Delta)\left(\theta(t)\Delta+\sigma(t)\sqrt{\Delta}Z\right), \tag{B.5}$$

where $\log(M(t_0)) = r(t_0)B(t_0,t)$ depends on t. Therefore, $\log(M(t_0))$ is set to 0 and $r(t_0)B(t_0,t)$ can be added after the discretisation

Furthermore, for the logarithm of the money-market account, equation (B.4)), a similar integration for each step is done as in the case of the interest-rate, $r(t)$. Equation (B.4)) is rewritten to:

$$\begin{aligned} \log(M(t)) &= -r(t_0)B(t_0,t)-\int_{t_0}^{t}\theta(s)B(s,t)\mathrm{d}s-\int_{t_0}^{t}\sigma(s)B(s,t)\mathrm{d}W(s) \\ &= \frac{r(t_0)}{\alpha}(1-e^{-\alpha(t-t_0)})+\frac{1}{\alpha}\int_{t_0}^{t}\theta(s)(1-e^{-\alpha(t-s)})\mathrm{d}s+\frac{1}{\alpha}\int_{t_0}^{t}\sigma(s)(1-e^{-\alpha(t-s)})\mathrm{d}W(s) \\ &= \frac{r(t_0)}{\alpha}(1-e^{-\alpha(t-t_0)})+\frac{1}{\alpha}\int_{t_0}^{t}\theta(s)\mathrm{d}s-\frac{1}{\alpha}\int_{t_0}^{t}\theta(s)e^{-\alpha(t-s)}\mathrm{d}s+\frac{1}{\alpha}\int_{t_0}^{t}\sigma(s)\mathrm{d}W(s)-\frac{1}{\alpha}\int_{t_0}^{t}\sigma(s)e^{-\alpha(t-s)}\mathrm{d}W(s) \\ &= \frac{1}{\alpha}\left(r(t_0)+\int_{t_0}^{t}\theta(s)\mathrm{d}s+\int_{t_0}^{t}\sigma(s)\mathrm{d}W(s)-r(t)\right) \end{aligned} \tag{B.6}$$

Where $\frac{1}{\alpha}\int_{t_0}^{t}\theta(s)\mathrm{d}s$ can be determined without Monte Carlo simulation. For $\int_{t_0}^{t}\sigma(s)\mathrm{d}W(s)$ the piecewise continuity of the $\sigma(t)$ is used and each step of the integral can be calculated by

$$\int_{t}^{t+\Delta}\sigma(s)\mathrm{d}W(s) = \sigma(t)\sqrt{t+\Delta-t}Z \tag{B.7}$$

B.1.3. Zero-coupon bond simulation

Remember, in equation (3.11) the affine form of the zero-coupon bond under the Hull-White model was given by

$$P(t,T) = e^{A(t,T)+B(t,T)r(t)}, \tag{B.8}$$

with

$$A(t,T) = \int_{t}^{T}\theta(s)B(s,T)\mathrm{d}s+\frac{1}{2}\int_{t}^{T}\sigma(s)^2B(s,T)^2\mathrm{d}s \tag{B.9}$$

$$B(t,T) = -\frac{1}{\alpha}\left(1-e^{-\alpha(T-t)}\right) \tag{B.10}$$

Now, $A(t,T)$ can be rewritten as:

$$\begin{aligned} A(t,T) &= \int_{t}^{T}\theta(s)B(s,T)\mathrm{d}s+\frac{1}{2}\int_{t}^{T}\sigma(s)^2B(s,T)^2\mathrm{d}s \\ &= -\frac{1}{\alpha}\left(\int_{t}^{T}\theta(s)\mathrm{d}s-e^{-\alpha T}\int_{t}^{T}\theta(s)e^{\alpha s}\mathrm{d}s\right)+\frac{1}{2\alpha^2}\left(\int_{t}^{T}\sigma^2(s)\mathrm{d}s-2e^{-\alpha T}\int_{t}^{T}\sigma^2(s)e^{\alpha s}\mathrm{d}s+e^{-2\alpha T}\int_{t}^{T}\sigma^2(s)e^{2\alpha s}\mathrm{d}s\right) \end{aligned} \tag{B.11}$$

B.2. Simulation Hull-White model zero mean-reversion

In this subsection, the money-market account and zero-coupon bond simulation with a zero mean-reversion parameter are discussed.

B.2.1. Money-market account simulation

Next, the money-market account, defined in equation (2.21), under the Hull-White model can be found by using equations (3.12),(3.24),(3.25) the closed form of the money market account is given by

$$\begin{aligned} M(t) &= \exp\left(\int_{t_0}^{t} r(s)\mathrm{d}s\right) \\ &= \exp\left(r(t_0)(t-t_0) + t\int_{t_0}^{T}\theta(s)\mathrm{d}s - \int_{t_0}^{T}\theta(s)s\mathrm{d}s + T\int_{t_0}^{T}\sigma(s)\mathrm{d}W(s) - \int_{t_0}^{T}\sigma(s)s\mathrm{d}W(s)\right) \\ &= \exp\left(-r(t_0)t_0 - \int_{t_0}^{T}\theta(s)s\mathrm{d}s - \int_{t_0}^{T}\sigma(s)s\mathrm{d}W(s) + tr(t)\right) \end{aligned} \tag{B.12}$$

B.2.2. Zero-coupon bond simulation

Remember, in equation (3.11) the affine form of the zero-coupon bond under the Hull-White model was given by

$$P(t,T) = e^{A(t,T)-B(t,T)r(t)}, \tag{B.13}$$

with

$$A(t,T) = \int_t^T \theta(s)B(s,T)\mathrm{d}s + \frac{1}{2}\int_t^T \sigma(s)^2 B(s,T)^2\mathrm{d}s \tag{B.14}$$

$$B(t,T) = -(T-t) \tag{B.15}$$

Now, $A(t,T)$ can be rewritten as:

$$A(t,T) = \int_t^T \theta(s)B(s,T)\mathrm{d}s + \frac{1}{2}\int_t^T \sigma(s)^2 B(s,T)^2\mathrm{d}s \tag{B.16}$$

$$\begin{aligned} &= -\int_t^T \theta(s)(T-s)\mathrm{d}s + \frac{1}{2}\int_t^T \sigma(s)^2(T-s)^2\mathrm{d}s \\ &= -T\int_t^T \theta(s)\mathrm{d}s + \int_t^T \theta(s)s\mathrm{d}s + \frac{1}{2}T^2\int_t^T \sigma(s)^2\mathrm{d}s - T\int_t^T \sigma(s)^2 s\mathrm{d}s + \frac{1}{2}\int_t^T \sigma(s)^2 s^2\mathrm{d}s \end{aligned} \tag{B.17}$$

C

Appendix C: Calibration Hull-White model

C.1. Hull-white model calibration to caplets

This section is a step wise description of the Calibration of the Hull-White model to caplets, which is given in Section 4.2.1.

The Hull-White model calibration uses the fact that a caplet payoff can be written as a put on a zero-coupon bond. More precisely, for expiry time T_i and $\tau_i = T_{i+1} - T_i$ (adjusted to the day count convention), the transformation is given by

$$\begin{aligned}
V_i^{\text{cpl}}(t,T_i,T_{i+1}) =& NM(t)\mathrm{E}\left[\frac{1}{M(T_{i+1})}\tau_i \max(F(T_i,T_i,T_{i+1})-K,0)\middle|\mathscr{F}_t\right]\\
=& NM(t)\mathrm{E}\left[\frac{1}{M(T_i)}\mathrm{E}\left[\frac{M(T_i)}{M(T_{i+1})}\tau_i \max(F(T_i,T_i,T_{i+1})-K,0)\middle|\mathscr{F}_{T_i}\right]\middle|\mathscr{F}_t\right]\\
=& NM(t)\mathrm{E}\left[\frac{1}{M(T_i)}\mathrm{E}^{T_i}\left[P(T_i,T_{i+1})\tau_i \max(F(T_i,T_i,T_{i+1})-K,0)\middle|\mathscr{F}_{T_i}\right]\middle|\mathscr{F}_t\right]\\
=& NM(t)\mathrm{E}\left[\frac{1}{M(T_i)}P(T_i,T_{i+1})\tau_i \max\left(\frac{1}{\tau_i}(\frac{P(T_i,T_i)}{P(T_i,T_{i+1})}-1)-K,0\right)\middle|\mathscr{F}_t\right]\\
=& NM(t)\mathrm{E}\left[\frac{1}{M(T_i)}\max\left(1-P(T_i,T_{i+1})(1+\tau_i K),0\right)\middle|\mathscr{F}_t\right]\\
=& N(1+\tau_i K)M(t)\mathrm{E}\left[\frac{1}{M(T_i)}\max\left(\frac{1}{1+\tau_i K}-P(T_i,T_{i+1}),0\right)\middle|\mathscr{F}_t\right]\\
=& N(1+\tau_i K)P(t,T_i)\mathrm{E}^{T_i}\left[\max\left(\frac{1}{1+\tau_i K}-P(T_i,T_{i+1}),0\right)\middle|\mathscr{F}_t\right] \qquad \text{(C.1)}
\end{aligned}$$

Where in the third line a change of measure from the risk neutral measure $\mathbb{Q}$ to the T_i-forward measure $\mathbb{Q}^{T_i}$ is used.

It follows that

$$V_i^{\text{CPL}} = (1+\tau_i K)V_{\text{put}}^{\text{zcb}}(t,T_i,T_{i+1},\frac{1}{1+\tau_i K}) \qquad \text{(C.2)}$$

$$V_{\text{put}}^{\text{zcb}}(t,T_i,T_{i+1},X) = NP(t,T_i)\left(X\Phi(-d_-^{\text{zcb}}) - P(t,T_i,T_{i+1})\Phi(-d_+^{\text{zcb}})\right) \qquad \text{(C.3)}$$

$$d_\pm^{\text{zcb}} = \frac{\ln(\frac{P(t,T_i,T_{i+1})}{X}) \pm \frac{1}{2}\text{Var}[P(T_i,T_{i+1})|\mathscr{F}_t]}{\sqrt{\text{Var}[P(T_i,T_{i+1})|\mathscr{F}_t]}} \qquad \text{(C.4)}$$

Now, to find the volatilities for the Hull-White model, first, the caplet price is calculated, using the market-implied volatilities. This caplet price is used to find the variance of the zero-coupon bond in equation (C.4). Hereafter, to find the Hull-White volatilities, σ_i, each market zero-coupon bond variance is set equal to the closed form of this zero-coupon bond variance under the Hull-White model, equation (3.19).

Therefore, the objective function is stated as:

$$\begin{aligned}
\text{Var}[P(t_0,T_i,T_{i+1},\alpha,\sigma_i)] &= \sigma^{\text{zcb}}_{mkt}(t_0,T_i,T_{i+1},K)^2(T_i-t_0)\\
\text{Var}\left[r(T_i)|\mathscr{F}_{t_0}\right]B(T_i,T_{i+1})^2 &= \sigma^{\text{zcb}}_{mkt}(t_0,T_i,T_{i+1},K)^2(T_i-t_0)\\
B(T_i,T_{i+1})^2\int_{t_0}^{T_i}\sigma^2(s)e^{-2\alpha(T_i-s)}\text{d}s &= \sigma^{\text{zcb}}_{mkt}(t_0,T_i,T_{i+1},K)^2(T_i-t_0)\\
\sum_{k=1}^{i}\frac{\sigma_k^2}{2\alpha}\left(e^{-2\alpha(T_i-T_k)}-e^{-2\alpha(T_i-T_{k-1})}\right) &= \frac{\sigma^{\text{zcb}}_{mkt}(t_0,T_i,T_{i+1},K)^2(T_i-t_0)}{B(T_i,T_{i+1})^2}
\end{aligned} \tag{C.5}$$

In equation (C.5), the summation is a result of the fact that for a given period $\sigma(t)$ is piecewise constant. Moreover, the summation can be rewritten as

$$\frac{\sigma_i^2}{2\alpha}\left(1-e^{-2\alpha(T_i-T_{i-1})}\right)+\sum_{k=1}^{i-1}\frac{\sigma_k^2}{2\alpha}\left(e^{-2\alpha(T_i-T_k)}-e^{-2\alpha(T_i-T_{k-1})}\right). \tag{C.6}$$

From which Hull-White volatilities, σ_i^2, can be found and are given by

$$\sigma_i^2=\frac{\frac{\sigma^{\text{zcb}}_{mkt}(t_0,T_i,T_{i+1},K)^2(T_i-t_0)}{B(T_i,T_{i+1})^2}-\sum_{k=1}^{i-1}\frac{\sigma_k^2}{2\alpha}\left(e^{-2\alpha(T_i-T_k)}-e^{-2\alpha(T_i-T_{k-1})}\right)}{\frac{1}{2\alpha}\left(1-e^{-2\alpha(T_i-T_{i-1})}\right)} \tag{C.7}$$

Global optimisation:

$$\min\sum_{i=1}^{n}\left[\sigma^{\text{zcb}}_{mkt}(t_0,T_i,T_{i+1},K)^2(T_i-t_0)-B(T_i,T_{i+1})^2\sum_{k=1}^{i}\frac{\sigma_{hw}(T_{k-1},T_k)^2}{2\alpha}\left(e^{-2\alpha(T_i-T_k)}-e^{-2\alpha(T_i-T_{k-1})}\right)\right]^2 \tag{C.8}$$

Zero mean-reversion Moreover, the calibration of the Hull-White volatilities, given in equation (4.14), for zero-mean reversion can be found using the zero-coupon bond variance in equation (3.26), which gives

$$\text{Var}\left[r(S)|\mathscr{F}_t\right](T-S)^2=\sigma^{\text{zcb}}_{mkt}(t_0,T_i,T_{i+1},K)^2(T_i-t_0) \tag{C.9}$$

Henceforth, the Hull-White volatility becomes

$$\sigma_i^2=\frac{\frac{\sigma^{\text{zcb}}_{mkt}(t_0,T_i,T_{i+1},K)^2(T_i-t_0)}{(T_{i+1}-T_i)^2}-\sum_{k=1}^{i-1}\sigma_k^2(T_k-T_{k-1})}{T_i-T_{i-1}} \tag{C.10}$$

C.2. Jamshidian decomposition

The Jamshidian decomposition given in equation (C.19-C.20) is derived as follows:

$$\begin{aligned}
V^{\text{swpt}}(t_0,T_i,T_n) &= P(t_0,T_i)\mathbb{E}^{T_i}\left[\max\left(V^{\text{swap}}(T_i,T_i,T_n),0\right)\middle|\mathscr{F}(t_0)\right]\\
&= NP(t_0,T_i)\mathbb{E}^{T_i}\left[\max\left(P(T_i,T_i)-P(T_i,T_{n+1})-K\sum_{k=i}^{n}\tau_kP(T_i,T_{k+1}),0\right)\middle|\mathscr{F}(t_0)\right]\\
&= NP(t_0,T_i)\mathbb{E}^{T_i}\left[\max\left(1-\sum_{k=i}^{n}c_kP(T_i,T_{k+1}),0\right)\middle|\mathscr{F}(t_0)\right]\\
&= NP(t_0,T_i)\mathbb{E}^{T_i}\left[\max\left(1-\sum_{k=i}^{n}c_ke^{A(T_i,T_{k+1})-B(T_i,T_{k+1})r(T_i)},0\right)\middle|\mathscr{F}(t_0)\right]
\end{aligned} \tag{C.11}$$

with $c_k=K\tau_k$ for $k=i,\ldots,n-1$ and $c_n=1+K\tau_n$. Hereafter, Jamshidian's trick is used. First, consider the monotonically increasing function [24].

$$A=\max\left(B-\sum_k\phi_k(r),0\right) \tag{C.12}$$

Then find a value r^* such that

$$B=\sum_k\phi_k(r^*) \tag{C.13}$$

Next we find by substituting

$$\begin{aligned} A &= \max\left(\sum_k \phi_k(r^*) - \sum_k \phi_k(r), 0\right) \\ &= \max\left(\sum_k \left(\phi_k(r^*) - \phi_k(r)\right), 0\right) \\ &= \sum_k \left(\phi_k(r^*) - \phi_k(r)\right) 1_{r>r^*} \\ &= \sum_k \max\left(\phi_k(r^*) - \phi_k(r), 0\right) \end{aligned} \tag{C.14}$$

Finally, applying Jamshidian's trick

$$\max\left(1 - \sum_{k=i}^{n} e^{A(T_i,T_{k+1}) - B(T_i,T_{k+1})r(T_i)}, 0\right) = \sum_k \max\left(e^{A(T_i,T_{k+1}) - B(T_i,T_{k+1})r^*} - e^{A(T_i,T_{k+1}) - B(T_i,T_{k+1})r(T_i)}, 0\right) \tag{C.15}$$

and r^* can be found by

$$\sum_{k=i}^{n} c_k e^{A(T_i,T_{k+1}) - B(T_i,T_{k+1})r^*} = 1 \tag{C.16}$$

Now

$$V^{\text{swpt}}(t_0) = NP(t_0,T_i) \sum_{k=i}^{n} c_k \mathbb{E}^{T_i}\left[\max\left(e^{A(T_i,T_{k+1}) - B(T_i,T_{k+1})r^*} - e^{A(T_i,T_{k+1}) - B(T_i,T_{k+1})r(T_i)}, 0\right) | \mathscr{F}(t_0)\right] \tag{C.17}$$

Concluding

$$\begin{aligned} V^{\text{swpt}}(t_0,T_i,T_n) &= NP(t_0,T_i) \sum_{k=i}^{n} c_k V_p^{\text{zcb}}(t_0,T_i,T_{k+1},X_{i,k}) \\ c_k &= K\tau_k \\ c_n &= 1 + K\tau_n \\ X_{i,k} &= e^{A(T_i,T_{k+1}) - B(T_i,T_{k+1})r^*} \end{aligned} \tag{C.18}$$

C.3. Hull-White model calibration to swaptions

Again, the mean-reversion parameter,α, is assumed to be given as an input, and the volatilities will be piecewise constant as described in Figure 4.1. The swaptions used for calibration have the following properties:

1. The used swaptions have maturity dates $T_i \in \{T_1, \ldots, T_n\}$
2. The maturity of the underlying swap, T_n, of the swaptions are determined depending on the products in the portfolio
3. Strike price K is ATM

The formulations given in [15] for the calibration of the Hull-White model to swaptions will be followed. A (payer) swaption with strike K, swap fixing dates $T_0, \ldots, T_n$ can be rewritten to a weighted sum of zero-coupon bond put options by Jamshidian's decomposition [24] and is given by

$$\begin{aligned} V_{\text{swpt}}(t_0,T_i,T_n,T_n) &= \sum_{k=i}^{n} c_k V_p^{\text{zcb}}(t_0,T_i,T_{k+1},X_{i,k}) \\ c_k &= K\tau_k \\ c_n &= 1 + K\tau_n \\ X_{i,k} &= \exp\left(A(T_i,T_{k+1}) - B(T_i T_{k+1})r^*\right) \end{aligned} \tag{C.19}$$

and where r^* can be found by

$$\sum_{k=i}^{n} c_i \exp\left(A(T_i,T_{k+1}) - B(T_i,T_{k+1})r^*\right) = 1 \tag{C.20}$$

For more details on the Jamshidian's decomposition we refer to appendix C.2.

Moreover, this sum is approximated and the variance of a swap rate, $S_{i,m,n}(t)$, can be rewritten to [15]

$$\text{Var}\left[S_{i,n,n}(t_0)\right] = \left(\frac{P(t_0,T_i)}{P(t_0,T_i) - P(t_0,T_n)}\right)^2 \text{Var}\left[P(t_0,T_i,T_{i+1},\alpha,\sigma_{hw})\right] \tag{C.21}$$

Note, that the swaption maturity is given by T_i and the swap tenor, swap length, is given by T_n. Where the T_i can be used to bootstrap the Hull-White volatilities and T_n is to be chosen. The swap tenors are often chosen with the co-terminal property, where all swap tenors are chosen such that all swaps end on the same date. The co-terminal depends on the portfolio that needs to be simulated.

D

Appendix D: Multi-curve framework

This appendix shows a multi-curve setting for equation (4.9) and how to rewrite this to only a forecasting curve. In the following equations, a change to the $T_i^{f_j}$-forward measure is used with $P^{f_j}(0,t)$ as numeraire with $f_j \in \{1M, 3M, 6M, 12M\}$:

$$
\begin{aligned}
V_{mkt}^{\text{cpl}}(t,T_i,T_{i+1}) &= N_i M(t)\mathrm{E}\left[\frac{1}{M(T_{i+1})}\tau_i \max(F(T_i,T_i,T_{i+1})-K,0)\middle|\mathscr{F}_t\right] \\
&= N_i M(t)\mathrm{E}\left[\frac{1}{M(T_i)}\mathrm{E}\left[\frac{M(T_i)}{M(T_{i+1})}\tau_i \max(F(T_i,T_i,T_{i+1})-K,0)\middle|\mathscr{F}_{T_i}\right]\middle|\mathscr{F}_t\right] \\
&= N_i M(t)\mathrm{E}\left[\frac{1}{M(T_i)}\mathrm{E}^{T_i^{f_j}}\left[P^{f_j}(T_i,T_{i+1})\tau_i \max(F(T_i,T_i,T_{i+1})-K,0)\middle|\mathscr{F}_{T_i}\right]\middle|\mathscr{F}_t\right] \\
&= N_i M(t)\mathrm{E}\left[\frac{1}{M(T_i)}P^{f_j}(T_i,T_{i+1})\tau_i \max\left(\frac{1}{\tau_i}\left(\frac{P^{f_j}(T_i,T_i)}{P^{f_j}(T_i,T_{i+1})}-1\right)-K,0\right)\middle|\mathscr{F}_t\right] \\
&= N_i(1+\tau_i K)M(t)\mathrm{E}\left[\frac{1}{M(T_i)}\max\left(\frac{1}{1+\tau_i K}-P^{f_j}(T_i,T_{i+1}),0\right)\middle|\mathscr{F}_t\right] \\
&= N_i(1+\tau_i K)P^{f_j}(t,T_i)\mathrm{E}^{T_i^{f_j}}\left[\max\left(\frac{1}{1+\tau_i K}-P^{f_j}(T_i,T_{i+1}),0\right)\middle|\mathscr{F}_t\right] \qquad \text{(D.1)}
\end{aligned}
$$